



Evaluation of acoustic emission for monitoring wire drawing process

Enrique Caso ^{*}, Alberto Diez-Ibarbia, Pablo Garcia, Javier Sanchez-Espiga, Alfonso Fernandez-del-Rincon

Department of Structural and Mechanical Engineering, ETSIT University of Cantabria, Spain

ARTICLE INFO

Communicated by J. JC

Keywords:

Acoustic emission
Wire drawing
Process monitoring

ABSTRACT

Acoustic emission (AE) technology is sensitive to high frequency waves generated in physical mechanisms as friction contact and plastic deformation, both present in the wire drawing process. In this regard, experimental measurements with this technology have been conducted to wire drawing in an industrial environment, in order to prove the technology validity to monitor this manufacturing process. The correlation of the results with the parameters defining the operation (as drawing speed, die temperature or lubricant type) and production (e.g. wire diameter, die status or incidences) intends to establish the main aspects to develop a correct monitoring for this application. Due to the complexity of the wire drawing and the interrelated parameters, tendencies in AE signal have been assessed under certain conditions in base to the experimental results. The study developed in tests with controlled-parameters for same single wire reel reveals a clear correlation between AE amplitude and lubricant chemical composition, as well as between AE amplitude and die temperature. Furthermore, the employment of another wire material or different die set makes the analysis more complex, revealing AE spectral variations and patterns that reflect slight changes of the process.

1. Introduction

Wire drawing is a complex cold metal-forming process, therefore, its monitoring is convenient to control product quality and drawing die degradation as well as to minimize incidents. Through monitoring, Industry can improve its manufacturing processes by early identification of deviations from good performance, which in turn, can lead to severe problems. As a result, productivity could be improved optimizing operating conditions with respect to unmonitored operation. Adequate monitoring prevents the progression of damage and consequent downtime for maintenance, resulting in a reduction of time and resources losses.

Several monitoring techniques have been studied for wire drawing application, focusing on quality control, defect identification and indirect detection from other process malfunctions. In the case of surface defects, inspection systems based on eddy currents are able to find flaws without contact by the use of induced currents after the wire cross-section reduction [1–3]. To maintain a correct lubricant impregnation of the wire is crucial to reduce friction and wear that can lead to failure. In this regard, the measurement of electrical resistance in the lubricant layer has been analysed as an indicator to detect inadequate lubrication [4,5]. On the other hand, tensile strength is also linked to friction and plastic deformation of the wire, being proposed its estimation through the capstan electric motor variables [6]. Likewise, recent approaches have considered the vibration analysis as monitoring tool for wire drawing [7]. Moreover, another approach proposes to improve the vibration detection capability by fusion with image processing

^{*} Corresponding author.

E-mail address: casoe@unican.com (E. Caso).

<https://doi.org/10.1016/j.ymssp.2023.110598>

Received 17 February 2023; Received in revised form 30 May 2023; Accepted 7 July 2023

Available online 24 July 2023

0888-3270/© 2023 The Author(s). Published by Elsevier Ltd. This is an open access article under the CC BY-NC-ND license (<http://creativecommons.org/licenses/by-nc-nd/4.0/>).

parameters [8]. In that case, image processing is focused on the wire surface characteristic after section reduction, controlling variations in reflection intensity [9] and identifying temperature gradients by means of thermographic images [10].

Acoustic Emission (AE) sensor technology is a potential candidate for monitoring wire manufacturing, due to the valuable information about drawing status contained in the high frequency signals, reflected in patents [11,12] and its application in industry [13]. Regardless these patents and the industry's interest, the literature on the AE monitoring of this process is scarce, with few studies on the subject [14,15]. However, due to the relation among AE and friction as well as contact phenomena and plastic deformation when a material is subjected to permanent alteration of shape, phenomena occurring in wire drawing, it has been subject of study for several manufacturing processes and machine tools, as cutting [16–18], drilling [19,20], grinding [21–24], milling [25,26], turning [27–29] or metal forming [30–33]. This monitoring is based on the information that can be extracted from the signals related to roughness in sliding friction [34]. On that basis, wear in the active surfaces can be assessed through AE generated in plastic and elastic deformation involved in friction mechanisms [35–37].

In the same way, the wire drawing involves physical mechanisms related with the contact of two bodies under stress, which is susceptible of generating AE. In wire drawing, AE has two main sources during the wire displacement: plastic and elastic deformation [15]. Firstly, plastic deformation due to the wire cross-section reduction generates sudden AE from the dislocations movement inside the material during its elongation. Secondly, the AE due to the elastoplastic deformation caused by asperity contact in the friction interface wire-die. Furthermore, adhesive and abrasive wear involve AE generation mechanisms [38]. Consequently, modifications of these phenomena could have a noticeable effect on the resulting AE signals, allowing accurate monitoring with this sensor technology.

In light of this complex process, with multiple and interconnected variables, the main aim of this work is to evaluate the sensitivity of AE for the wire drawing characterization, in order to prove its validity in the monitoring of this manufacturing process. After this introduction, the fundamentals and industrial specifics of the wire drawing manufacturing process are detailed in Sections 2 and 3. Then, the monitoring parameters as well as the signal processing are described in Section 4. Next, the description and the results of the experimental tests are presented in Sections 5 and 6. Finally, the conclusions of this work are outlined in Section 7.

2. AE in wire drawing: wire and die interaction

The AE generation in the wire drawing process depends, *inter alia*, on the tribological behaviour in the contact area. That interaction involves several components and layers consisting of die, wire, wire coating, lubricant and lubricant-coat reacted compounds (Fig. 1).

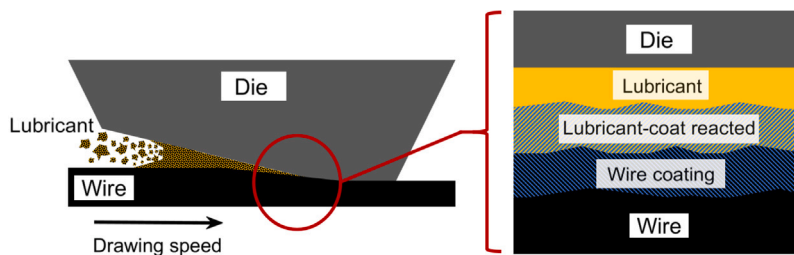


Fig. 1. Scheme of the layers in the interaction area.

Active surfaces interaction takes place under boundary lubrication, therefore, friction is controlled by the chemical properties of the lubricant rather than its viscosity [39]. In the interaction area, the lubricant reacts with the coated wire surface producing a half-way material softer than wire and die. As a result of this, lubricant, die and wire material interfere in the contact, affecting the AE generation sources [14]. This boundary lubrication performance varies with process parameters instabilities, being worse during starts and stops, at low speed (if the necessary pressure to introduce sufficient lubricant is not achieved), when the load is excessive (overcoming the separating effect of the lubricant) or due to other aspects (e.g. due to wire/die poor surface characteristics or due to lubricant degradation). Inadequate boundary lubrication increases the wear of the die and the possibility of wire breakage.

The most usual main component of the wire drawing lubricant is a fatty acid soap, combined with other additives to modify its properties [40]. These dry soap type lubricants can be classified according to their solubility in water, establishing two main categories:

- (a) Calcium soap (insoluble): fatty acid + lime \rightarrow calcium soap + H_2O
- (b) Sodium soap (soluble): fatty acid + caustic soda \rightarrow sodium soap + H_2O

Calcium-based soap is recommended for the early stages, while sodium soap is used in the later stages where the wire reaches higher speeds and stresses [41]. Sodium soaps are more fluid than calcium soaps [42] and therefore favour conditions closer to hydrodynamic lubrication than calcium soap. Another consequence of the soap properties is that the shear stresses in the wire are lower using sodium than calcium soap [41].

The wire can be surface-treated according to the desired specifications with a coating, mainly zinc phosphate, to minimize friction in the process [43]. However, this phosphate coating can be delaminated depending on the steel composition, the geometry of the die or lubricant chemical composition. The role of this layer is important during lubrication as the powdered lubricant adheres to it, being better if the particles are small [44].

Die active surface topography must remain smooth to avoid the friction coefficient increment and the subsequent heating of the interface [45]. The die is made of a hard material, generally wolfram carbide (WC), whose surface is subject to abrasive and adhesive wear. Therefore, the die topography can be deteriorated resulting as a source of scratches and progressive phenomena, leading to wire surface damage. Additionally, high hardness particles detached from die wear produce abrasion when the wire pass through.

During wire drawing, friction and plastic deformation contributes to heat the contact area. On the one hand, an increase in temperature reduces the stress flow in the wire and the force required for drawing [46], because the higher the temperature is, the lower the yield strength value. The AE emitted due to the plastic deformation of the material depends on the zone of the stress-strain curve in which it is located [47,48] and would be mainly due to the effect of dislocations [31].

The heat produced in the process also increase the die temperature. This temperature increment results into die thermal expansion, modifying the wire nominal diameter. Therefore, die thermal effects have an effect on the quality of the resulting wire [49] and on a hardness reduction of die surface that favours its degradation [50]. The cooling system, mostly present in drawing lines, is effective in reducing the die abrasion [51]. Thus, improved surface conditions are obtained avoiding uncontrolled heating, hence providing a better wire quality [52] and die life time.

The third effect of the heat involves the lubricant properties variation with temperature. Excessive temperature of the wire affects the impregnated soap, supposing a greater problem for the process than the heating of the die itself [53]. The lubricant is affected, degraded under extreme conditions, reacting with the wire surface or changing its viscosity and wettability. The dimensional change properties of the lubricant are affected above 100 °C for both calcium and sodium soaps. The efficient operating range for calcium stearate, classified as a calcium soap, reaches 300 °C and does not fail completely until surpassing 400 °C [46].

3. Description of the drawing line and its operation

This work has been performed in an industrial wire drawing facility, monitoring a production line without significant modifications to normal procedure. Therefore, the obtained results are adequate to validate the implementation of the AE monitoring in real environment. This working condition imposes several limitations to the experiment set-up definition due to the manufacturing process schedule and the control of changes in the monitored line and auxiliary elements. Nevertheless, the tests have been performed with the aim of minimizing possible deviations in the operational parameters.

The monitoring target is the last stage die of a multi-stage wire drawing line (Fig. 2), due to its propensity to incidences because of the minor wire section and maximum speed.

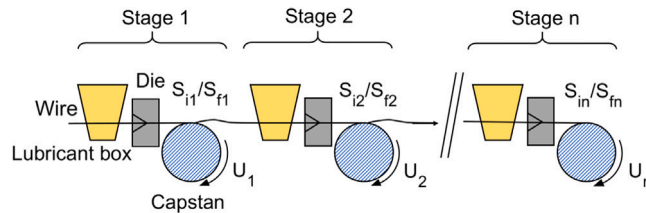


Fig. 2. Scheme of the multi-stage drawing line.

Each of the 8 stages is composed by the same components, being the main elements the capstan, the lubricant box and the die box (containing the die). The global cross-section reduction between initial and final section (S_i/S_f) imposed to the wire is obtained with the partial reduction in all stages (S_{i1}/S_{f1} , S_{i2}/S_{f2} , ... S_{in}/S_{fn}). In this application case, this global cross-section reduction (S_i/S_f) is between 2 and 2.4.

The employed dies, composed of a wolfram carbide core, are specifically selected for the desired wire reduction, which in turn corresponds to a specific wire product according to the industry standards. Therefore, when a modification of the wire reduction is performed, every die geometry in the previous stages to the monitored one (last stage) are modified accordingly. Thus, the global wire reduction is distributed over the entire line.

The die boxes (Fig. 3(a)) are placed between two capstans, releasing and drawing the wire, where the speed and temperature of the wire are measured using the line built-in sensors (pyrometer and tachometer). Therefore, input and output values, before and after cross-section reduction, are registered.

One wire product is divided in several length sections, denominated “reel”, that are rolled and packed to facilitate its handling and transportation. Whenever this sections are drawn consecutively, same working conditions can be assumed. Temperatures in the wire and die may vary, exhibiting a transitory related to the start and stop of the process. Nevertheless, temperature equilibrium is reached at similar values without significant dispersion. Consequently, AE should maintain similar signal levels meanwhile the process and the involved components remain in good conditions.

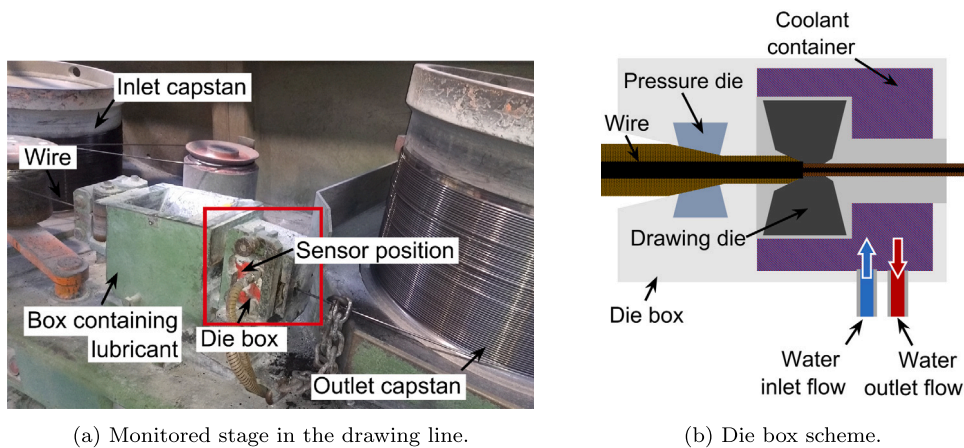


Fig. 3. Drawing line and die box components diagram.

Previously the wire goes through the die box, it is impregnated with dry lubricant by its immersion in the lubricant box. During these tests, the employed dry soap correspond to a calcium-based lubricant (CONDAT product ref. TF 124) suitable for high carbon and stainless steel, but also to a sodium-based soap (CONDAT product ref. SUMAC 3*), indicated for high performance requirements. Lubricant type can be replaced, substituting the soap powder in the containing boxes located before each stage die box.

This die box configuration (Fig. 3(b)) contains both the pressure die, that provides the adequate amount of lubricant, and the drawing die, that performs the cross-section reduction. The drawing-die-temperature is indirectly measured at the external surface of the die box (18–35 °C range during standard operation). Overheating is controlled by an alarm activation above 40 °C. That temperature is controlled with the cooling system by heat transfer to a water flow circulating around the die. This flow can be closed actioning the inlet duct valve.

The drawing line is operated controlling the wire speed imposed by the capstan rotation. During standard drawing conditions, a stationary speed is selected for the whole wire reel, except the initial and final transitory. These stationary conditions are set in advance for each specific wire, according to its section reduction, surface coating and other material characteristics. In other words, for the same wire product, if speed, lubricant and wire surface properties remain with minor modifications, incidences are not expected and, therefore, the reel is continuously drawn until the pre-set length is fulfilled.

The standard operating conditions of this drawing line is to use calcium-based soap, and the wire speed is generally between 4–7 m/s. For especial conditions, such as the need of a better performance in the last stages (high performance products) or when posterior surface treatment is applied (electrodeposition), the sodium-based soap is utilized, which in turn modifies the wire speed in a range of 6–7 m/s. Additionally, when the operation is initialized after set or maintenance stoppages, the wire drawing is started in a low speed range of 0.5–3 m/s.

4. Monitoring set-up

Initially, an analysis of the drawing line was performed in order to evaluate the parameters that could be controlled (Table 1) and the ones that could be monitored but out of our control (Table 2).

Table 1
Test control parameters and description.

Parameter	Description
Drawing speed	It can be modified to another stationary level allowing to study transitory effects
Lubricant	Contact conditions and lubrication regime can be modified by using a different chemical composition of the dry lubricant (calcium or sodium-based)
Die temperature	The contact interface thermal behaviour can be modified increasing the temperature through the control of the inlet water flow of the cooling system
Die surface characteristics	Die is subject to wear, hence, replacing it by a new one provides a healthy die but with different micro-surface characteristics

It must be taken into account that the modification or control of these parameters may have interrelated effects on the rest of the process variables.

In order to monitor the line, the built-in sensors controlled the wire speed, wire temperature and die temperature (measured in the die box external surface), and the AE sensor was installed in order to obtain information about the die surface characteristics

Table 2

Test uncontrolled parameters and description.

Parameter	Description
Die wear	The die tends to degradation, observed through wire nominal diameter deviation and corresponding wire damage
Wire temperature	Wire is cooled with air and in the capstans, but the resulting temperature after the section reduction depends in the wire-lubricant-die interaction
Unlubricated conditions	Incidences in the drawing process can lead to an incorrect impregnation and the subsequent wire galling
Wire breakage	The breakage can occur randomly during the drawing process

**Fig. 4.** Picture of the AE sensor positioned in contact with the die box using a magnetic holder.

and wear, lubrication conditions and wire breakage prevention. The employed sensor is a model *VS150-RIC* from *Vallen Systeme* with an adequate response up to 450 kHz and resonant frequency at 150 kHz.

The positioning of the sensor is determined by the space available and by ensuring that it is securely attached to prevent it from being damaged. Several positions in the die box were tested obtaining a coherent response for same stimulus in all of them, despite slight differences in the signals amplitude and spectrum. The AE sensor was placed in direct contact with the die box external surface (Fig. 4). The couplant degradation, with time and temperature, and the need to frequently remove the sensor and apply a new couplant layer (due to die-box removal every die replacement) would interfere in the results interpretation during this long-term monitoring. Due to the great uncertainty incorporated by the use of a couplant between sensor and surface, it has been decided to not use any couplant (decision contrasted with experimental tests).

The AE signals are acquired at sample rate of 1 MS/s using an acquisition board *AdLink USB-1210* with a developed LabVIEW application. As a result, big-size files are obtained, supposing 5 mb of memory storage for 1-second AE signal. File size is a limiting factor to implement a reliable continuous monitoring strategy if continuous signal acquisition is intended. For the selected monitoring approach, the signal record is automatically performed by the acquisition software, registering 1-second measurement each 2-min interval (Fig. 5). In certain cases, as in the register of a transitory effect of the speed, longer time acquisition signals have been recorded, maintaining the sample rate.

In spite of the non-continuous acquisition, the large size of the AE signal files leads to the use of signal processing tools that allows the handling of numerous records. In addition to the usual methods (for example, the RMS of the signal is used to represent the level of the AE), an indicator was defined to achieve an analysis of the monitoring in terms of AE spectral content while reducing the used data denominated “AE spectral indicator”. Fig. 6 displays the strategy used to define the AE spectral indicator, similar to the use of the RMS as an indicator from the time domain signal.

For the calculation of the AE spectral indicator, three bands were selected representing the low frequency (25–55 kHz), the medium frequency (55–150 kHz) and the high frequency (150–300 kHz). The middle and high bands separate the spectrum content below and above the resonant frequency of the sensor, with different sensitivity to the generated AE waves. In each of these bands, the delimited area below the spectrum is calculated by obtaining a value that is normalized to the RMS of the full signal according to Eq. (1). Therefore, the AE spectral indicator denotes the distribution of the spectral content in the frequency spectrum, obtaining

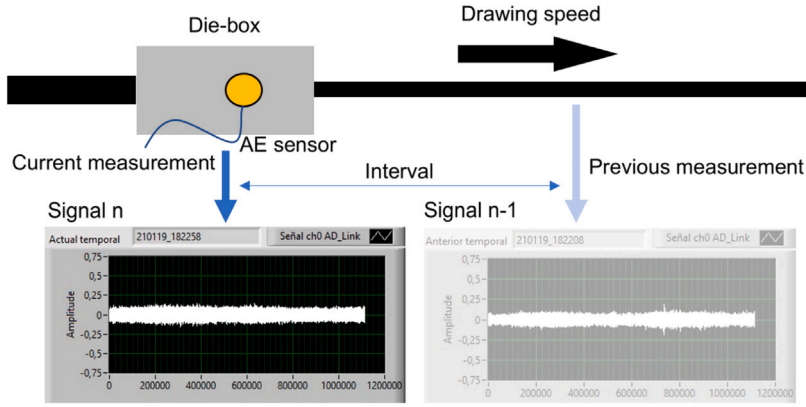


Fig. 5. Scheme of the monitoring approach with the AE signals.

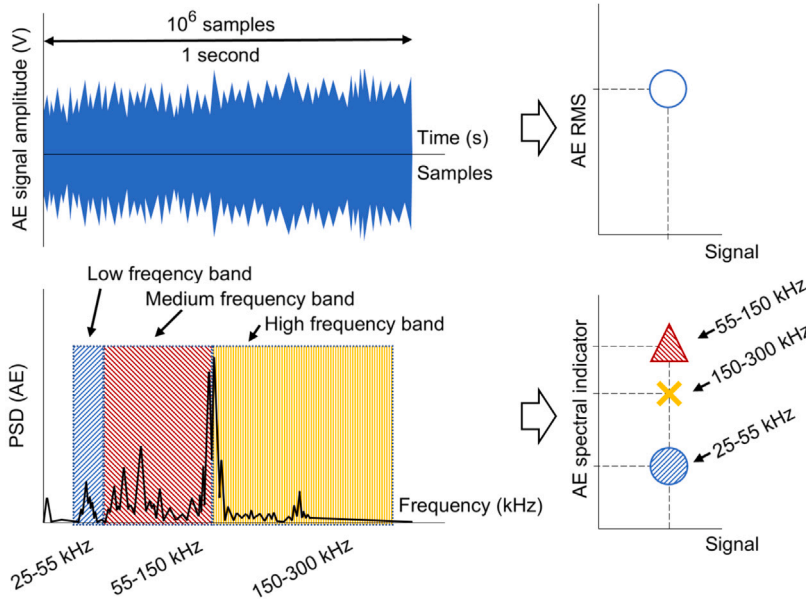


Fig. 6. Scheme of the AE signals processing.

three values, one for each band.

$$AE_{spt}^{freq.band} = \frac{\int_{f_1}^{f_2} PSD(V_{AE}) df}{RMS(V_{AE})} \tag{1}$$

where, V_{AE} corresponds to the AE signal in time domain, df is the differential frequency for the AE signal PSD integration between the frequency band $f_1 - f_2$ limits, obtaining the indicator AE_{spt} for low, mid and high frequency band.

These specific bandwidths (25–55, 55–150 and 150–300 kHz) were selected due to sensor specifications and their response to different wire drawing operational behaviours, which favoured the supervision of the acquisition system integrity. Comparing the main frequency band of the indicator, it was possible to check signals integrity in a simplified way, both for remote surveillance and on-site operators. Different bands content provides information about correct acquisition (in operation or during stoppage) or to detect abnormal sensor operation (several sensors were damaged), incorrect connections and power supply malfunctioning. Furthermore, the indicator has proven to be a tool with potential for the wire drawing process monitoring.

5. Description of the experimental tests

The experiments consist of acquiring acoustic emission signals during the operation of the wire drawing line, modifying some of the control parameters in each test, whilst the rest remain unchanged. The casting material employed for the wire production varies among the tests, hence just within the same reel or consecutive reels it can be considered same wire material.

Table 3

Defining parameters of the experimental tests (described in Section 5) performed in the industrial facilities (same drawing line).

Test Parameters	Surface contact conditions			Die temperature		Drawing die degradation		
	Test 1a	Test 1b	Test 1c	Test 2a	Test 2b	Test 3a	Test 3b	Test 3c
Same/different reel	Same	Same	Same	Same	Same	Different	Different	Different
Same/different reduction	Same	Same	Same	Same	Same	Same	Different	Different
Drawing speed (m/s)	2.5, 5.5 & 2.5–5.5	5.5	2.5, 5.5 & 6.5	6.5	5.5	5.5	~5.5	2.5, 5.5 & 6.5
Lubricant type	Calcium	1 st Calcium 2 nd Sodium 3 rd Calcium	1 st Calcium 2 nd Sodium 3 rd Calcium	Calcium	Calcium	Calcium	Calcium	Calcium
Refrigeration	Active	Active	Active	Cut-off	Cut-off	Active	Active	Active
Warning die temp. alarm	40 °C	40 °C	40 °C	40 °C	Deacti-vated	40 °C	40 °C	40 °C
Incidents	–	–	–	–	Delamina-tion	Breakage, Die wear	Breakage, Die wear	–

The performed experiments can be classified in three groups according the main goal studied in each one of them.

1. Surface contact conditions: Drawing speed is the main control parameter, affecting the sliding speed but also the volumetric deformation rate. Moreover, the lubricant type (its chemical composition) also has an effect in the sliding conditions.
2. Temperature effects: Higher (than standard) die temperature modifies lubricant working point and material properties.
3. Drawing die degradation: Drawing die replacement modifies the contact conditions due to different wire-product reduction or because surface degradation of current components (being obliged to replace it).

The parameters varied in each test (reel, reduction ratio, drawing speed, lubricant type and refrigeration conditions) are summarized in Table 3 and their description is detailed next:

Test 1a. Speed influence: Within the same wire reel and with the same reduction ratio and lubricant type, the line is actioned at two stationary drawing speeds selected for the experiments, 2.5 m/s (low speed) and 5.5 m/s (medium or nominal speed). That range is consistent with the values used by the industry and it can be considered representative of steel wire drawing production. Also speed transitory (2.5–5.5 m/s) is considered to evaluate the AE response. In this regard, several long duration 10-second AE signals are acquired to register the transient effect.

Test 1b. Lubricant influence: Within the same wire reel at stationary speed of 5.5 m/s and with the same reduction ratio, the lubricant type supplied by the last stage lubricant box is changed. The wire is drawn with a calcium-based soap that is replaced with a sodium-based and back again to calcium-based soap in order to ensure the results repeatability. The monitoring is performed acquiring periodic 1-second AE signals (2 min interval, see Fig. 5).

Test 1c. Speed and lubricant influence: Within the same wire reel and with the same reduction ratio, the lubricant type supplied by the last stage lubricant box is changed for three stationary drawing speeds of 2.5, 5.5 and 6.5 m/s. Therefore, an analogous methodology than the previous test is applied, dividing the reel in three lubrication phases, each one at the three selected speeds, first one with calcium-based lubricant, second with sodium-based and third repeating the calcium-based to assure the cause–effect relation between lubricant and AE signals variation. The AE signals of 1-second duration are periodically acquired (2 min interval, see Fig. 5).

Test 2a. Standard range die temperature influence: Within same wire reel, 1-second AE signals are acquired periodically (2 min interval, see Fig. 5) meanwhile the refrigeration is removed by cutting off the inlet flown of water that is cooling the die. The drawing speed and the rest of parameters remained constant to isolate the effect of the temperature increase in the AE signals. Previously the cut-off, the line is operated in stationary conditions to warm-up the system, avoiding initial perturbations.

Test 2b. Out-of-range die temperature influence: Within same wire reel, analogous methodology than previous test is followed but deactivating the alarm systems to allow the drawing line operation over 40 °C die temperature. Hence, refrigeration is removed by cutting off the inlet flown acquiring 1-second AE signals periodically (2 min interval, see Fig. 5). The operation over standard temperature limits reproduce a incident behaviour that leads to manufacture a damaged wire.

Test 3a. Influence of the reel: For several reels, successively drawn at same cross-section reduction ($S_i/S_f = 2.30$) and same stationary drawing speed of 5.5 m/s, the factory standard operation is monitored. The aim of this test is to analyse the AE signals during continuous operation. This continuous operation is prone to incidents (wire breakage, die wear, uncontrolled increase of the wire temperature and unlubricated conditions), leading to perform corrective maintenance activities that are registered and considered in the signal analysis. Hence, 1-second AE signals are periodically acquired every two minutes to supervise the process.

Test 3b. Influence of cross-section reduction: For several reels, successively drawn at different cross-section reduction ($S_i/S_f = 2.22, 2.30$ and 2.38) and (approximately) same stationary speed of 5.5 m/s, the line production is monitored in order to analyse this aspect in the AE. The monitoring of the standard operation in the factory is performed acquiring 1-second AE signals periodically every two minutes.

Test 3c. Influence of reel with different drawing speed: For several reels of different cross-section reduction and three controlled stationary speeds of $2.5, 5.5$ and 6.5 m/s, the effect in the AE of the speed variation is analysed considering two cross-section reduction and two reels for each one. Several long duration 10-second AE signals are acquired during these 4 reels manufacturing. Additionally, the AE signals periodically acquired during one month monitoring (2 min interval, see Fig. 5), drawn at several stationary speeds (4.3 – 6.1 m/s) and four cross-section reduction ($S_i/S_f = 2.22, 2.29, 2.30$ and 2.38) are utilized to evaluate the variation of these three parameters during the monitoring.

Additionally to these tests, another scenario (denominated in this work as “monitoring of standard production”) is considered as a representation of other aspects that can affect the behaviour of standard operation, but they are not considered in deep in the current study. One aspect is the variation of the casting wire material of which the reels are composed, supposing a modification in spite of the reels are successively drawn at same cross-section reduction ($S_i/S_f = 2.38$) and at same stationary drawing speed (6.5 m/s). Second aspect shown in this monitoring example is a severe progression of die wear (notified by inspection report) that leads to an incidence, considering both wire and die as damaged, and consequent production stoppage.

6. Results and discussion

The results of the study on the effect in AE signals, addressing the main parameters characterizing the wire drawing, are outlined below in three subsections that covers different aspects by the realization of several tests (described in previous Section 5).

6.1. Surface contact conditions and AE

6.1.1. Test 1a: Speed influence

The results obtained in Test 1a, varying the drawing speed within same reel, reveal that an increase of the drawing speed provokes a higher amplitude on the AE signals. This is shown in Fig. 7 where the time domain AE signal and its spectrum are displayed for two stationary speeds, 2.5 and 5.5 m/s, and the transitory between both levels.

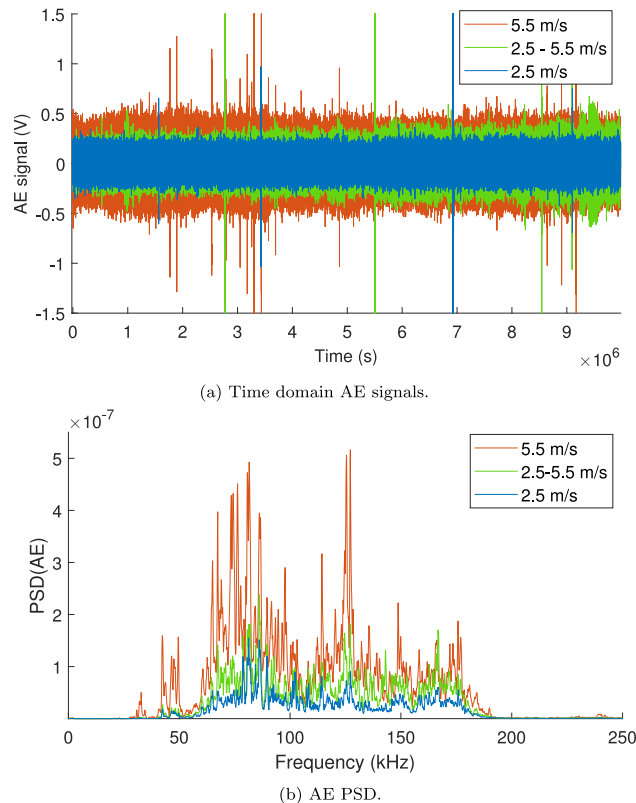


Fig. 7. Time and frequency AE content for two stationary drawing speeds, 2.5 and 5.5 m/s, and transitory from 2.5 to 5.5 m/s within same wire reel (Test 1a).

A transient increase (respectively decrease) of the drawing speed results in higher (respectively lower) AE amplitude in the time domain signals (Fig. 7(a)). Same response is obtained in the signal frequency domain observing three differenced levels, as is shown in Fig. 7(b), representing the power spectral density of same signals at 2.5, 5.5 and transitory 2.5–5.5 m/s. This amplitude increment is distributed along the frequency spectrum, obtaining same excited frequency peaks and bands, but higher for faster drawing.

The generalization of this result, correlating the speed level with AE amplitude, is only valid within the same reel. Although the speed increase supposes an augmentation of the rate and stress of the AE generation phenomena, due to sliding friction and volumetric deformation, the obtained response is consequent with this hypothesis in the close time when the speed variation is applied. Thus, the new stationary condition after the transitory does not imply a higher AE amplitude whenever the final speed is higher.

The validity of the speed range for the observed trend between AE amplitude and speeds seems to vary depending the characteristics of the reel and die status, variable with operation time. The drawing of different reels supposes modification of working conditions to be compared, several parameters that can affect in the AE must be considered, as the section reduction, wire roughness, wire casting, applied coating, die surface health or lubricant type. That aspect is shown in the following results of Test 3c, where different reels and different speeds are considered.

6.1.2. Test 1b: Lubricant influence

Test 1b evaluates the modification of the lubricant type (calcium or sodium-based) within the same reel at stationary speed of 5.5 m/s. Fig. 8 displays the spectral sequence of the AE signals when the lubricant supplied in the last stage die box is modified.

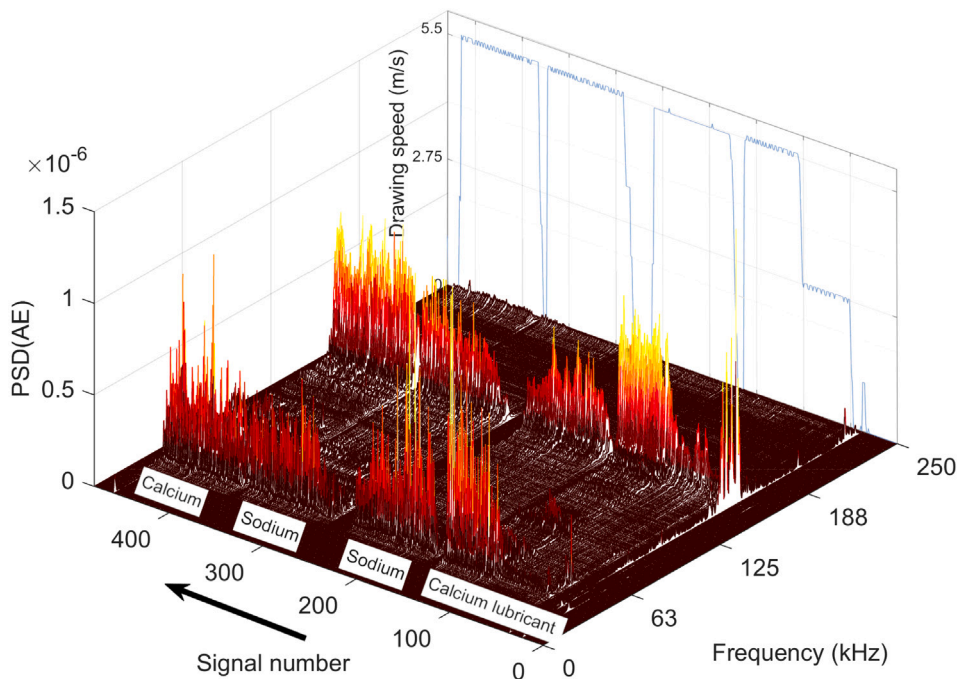


Fig. 8. AE spectral evolution using calcium and sodium lubricant during same reel drawing (Test 1b).

The AE spectrum shows higher amplitude peaks when the calcium-based lubricant is employed than when the sodium lubricant (Fig. 8). Frequency peak variation is more evident for the 150 kHz band, where the sensor exhibits its resonant frequency. Moreover, a peak in the low frequency band between 50–60 kHz is also affected with the lubricant type despite the lower sensor sensitivity. The test is divided in two phases, repeating the lubricant modification in inverse order. Firstly, starting by the sodium-based soap and changing to the calcium-based, and secondly, in reverse order, observing the same response for same lubricant.

The obtained results about the lubricant depends not only on its chemical composition but in the reactivity with the wire surface. That aspect controls the friction and the contact mechanisms generating part of the AE. That leads to perform an analogous test (Test 1c) in another reel from a different wire casting material to validate the results. In addition, an analysis of whether the drawing speed has an effect depending on the type of lubricant is considered, combining the lubricant change with several stationary speeds.

6.1.3. Test 1c: Speed and lubricant influence

Fig. 9 displays the time domain signals, when both the lubricant type and speed are modified. It is observed that the AE amplitude is higher for the sodium-based lubricant at the three considered stationary speeds of 2.5, 5.5 and 6.5 m/s.

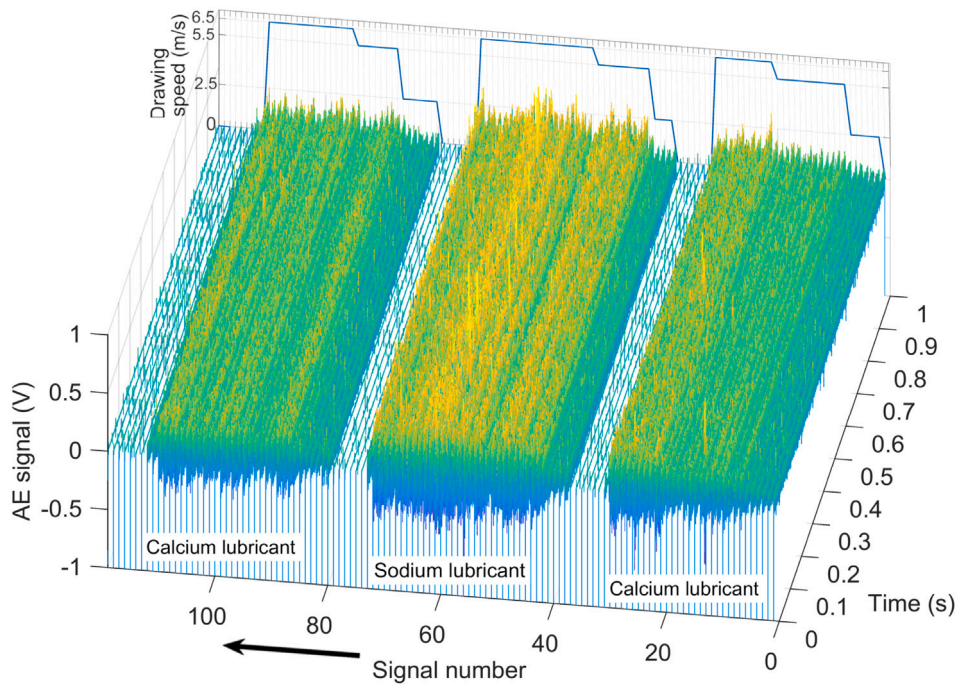


Fig. 9. AE time domain signals acquired during the drawing under different lubricant type (Test 1c).

The first aspect to consider of the Test 1c results is the opposite response in AE amplitude than the observed in Test 1b according to the lubricant. Nevertheless, the operation with different lubricant type, at same working conditions, remains distinguishable by variations in the AE signals. To assure that variations are due to the lubricant type, the drawing with calcium lubricant is repeated again after the second test phase with sodium lubricant, recovering similar values than in the first calcium lubricated phase of the test.

The frequency spectrum evolution of the AE signals with calcium and sodium-based lubricants is shown in Fig. 10 for each lubrication phase. Furthermore, the averaged spectrum of same speed signals is included in parallel to the PSD waterfall graph to display the pattern changes between lubricant type. When the sodium lubricant is employed the higher peak amplitude in the spectrum is obtained for all the considered speeds (Fig. 10(b)). Furthermore, the modification of the lubricant alters the spectral pattern formed by the main excited frequency peaks, as observed in the differences between Figs. 10(b) and 10(a)/10(c), where the AE displays higher low-frequency content for sodium-based lubricant.

Fig. 11 displays the RMS of the AE signals with both lubricants (same signals than Figs. 9 and 10).

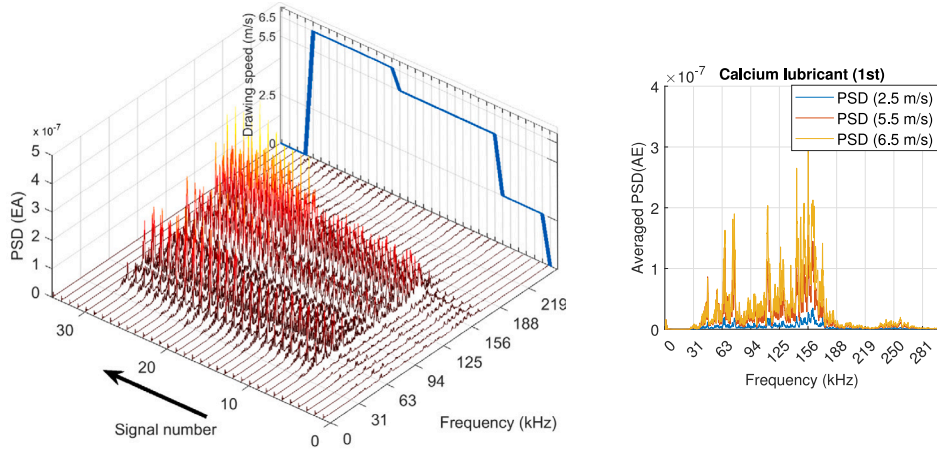
The linear interpolation reveals the different variation of AE with speed depending on which lubricant is used or, more precisely, on a relationship between the characteristics of the wire and lubricant. A tendency close to linearity in the relative variation amplitude-speed is obtained for the sodium-based lubricant. On the other hand, this relative variation in the AE amplitude for calcium type is closer to the square root of the drawing speed.

Lubricant working point, for same working conditions, imposes different contact behaviour for different chemical composition due to the reactivity in the boundary regime. Therefore, AE variations can be attributed to wire-die interface characteristics.

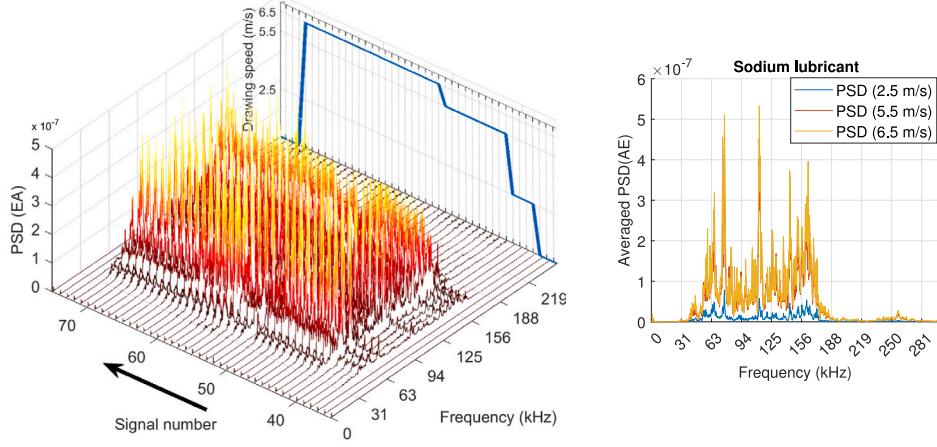
Although some tendencies were observed from the interpolation lines (Fig. 11), it was deemed interesting to analyse the AE signals in the frequency domain. In this analysis, some differences were observed in the spectral pattern depending on the lubricant type, which suggest that the AE response may vary according to the frequency range.

In this respect, three frequency bands were selected regarding the AE signal behaviour, low-frequency (25–55 kHz), mid-frequency (55–150 kHz) and high-frequency (150–300 kHz). The evolution of these bands is useful to analyse progress in successive signals. Moreover, an indicator based on the calculation of the spectral area under the spectrum in the defined frequency bands is employed to analyse the AE frequency distribution (Eq. (1)), which is shown in Fig. 12 for each speed (2.5, 5.5 and 6.5 m/s).

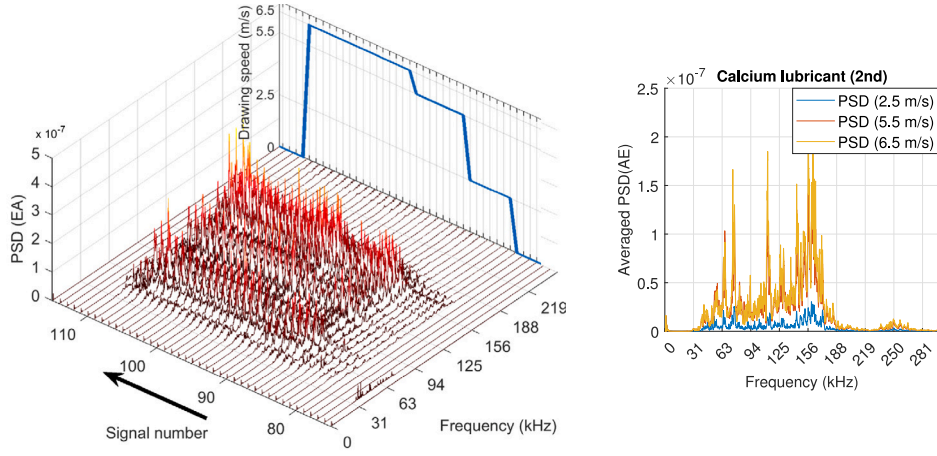
From the results it was observed that the AE low-frequency range, represented through $AE_{spt}^{25-55 \text{ kHz}}$, is significantly lower than the corresponding to the other two, independently of the speed and the lubricant type. Moreover, the $AE_{spt}^{55-150 \text{ kHz}}$ medium-frequency range is higher than the other two in all condition. Regarding the drawing speed, the higher speed the higher the AE amplitude, especially in the medium-frequency range. Regarding the lubricant type, sodium AE spectral indicator is higher than the corresponding to calcium (both cases), this aspect is even more significant in the medium-frequency band. As something to point out, AE is more sensitive in the medium frequency range to variations in speed and lubricant type.



(a) AE signals PSD for first calcium lubricant phase.



(b) AE signals PSD for sodium lubricant phase.



(c) AE signals PSD for second calcium lubricant phase.

Fig. 10. Spectral evolution of the AE signals with calcium and sodium lubricant for the three drawing speeds of 2.5, 5.5 and 6.5 m/s (corresponding to signals in Fig. 9, Test 1c).

Moreover, in order to improve the understandability of the results presented in Fig. 12, the increment of the spectral indicator (ΔAE_{spr}) with respect to the corresponding 2.5 m/s drawing speed are detailed in Table 4, expressed as fraction of unity. This

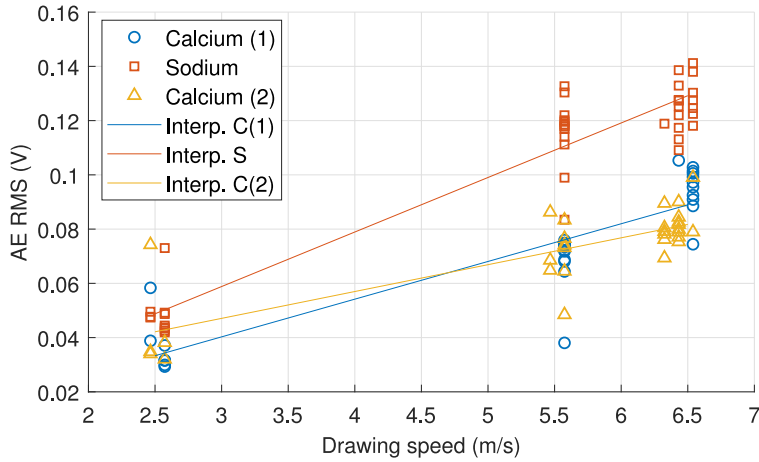


Fig. 11. AE RMS vs. drawing speed (Test 1c).

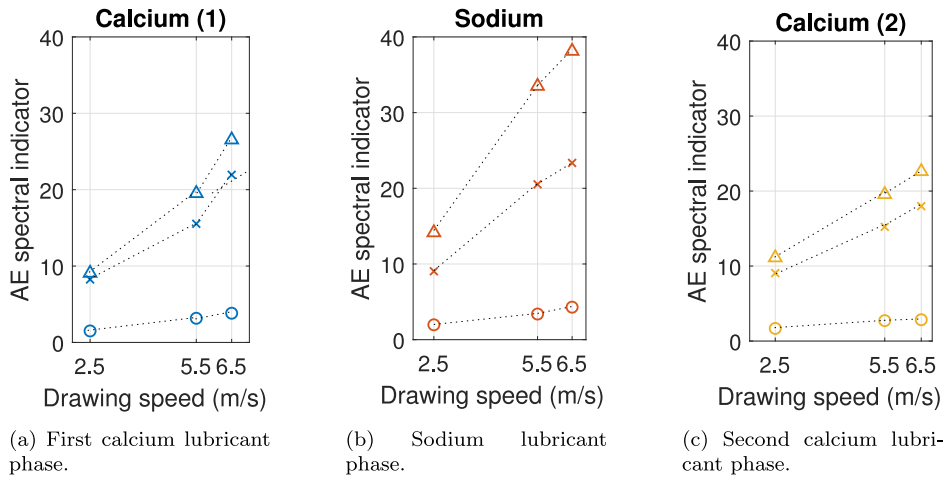


Fig. 12. AE spectral indicator vs. drawing speed by frequency band, where \circ corresponds to 25–55 kHz, \triangle to 55–150 kHz and \times to 150–300 kHz (Test 1c).

Table 4

Relative increment of AE spectral indicator with respect to the 2.5 m/s drawing speed for both lubricants (from same data than Fig. 12).

Lubricant	Calcium (1)		Sodium		Calcium (2)		
	Speed (m/s)	5.5	6.5	5.5	6.5	5.5	6.5
25–55 kHz		1.10	1.54	0.72	1.19	0.89	1.06
55–150 kHz		1.15	1.48	1.37	1.70	0.97	1.44
150–300 kHz		0.88	1.39	1.21	1.58	0.79	1.28

increment is calculated by Eq. (2).

$$\Delta AE_{spt} = \frac{AE_{spt}^{freq.band}|_v - AE_{spt}^{freq.band}|_{2.5}}{AE_{spt}^{freq.band}|_{2.5}} \tag{2}$$

where v is the drawing speed, in this case 5.5 and 6.5 m/s.

From the frequency band analysis with the spectral indicator, it can be observed that the higher the drawing speed, the higher the increment is. This effect is even more relevant in the medium frequency band, where this increment is higher than in the other two bands.

Although the AE RMS value tendency is to increase with the speed (Fig. 11), it is not so clear for all the RMS values. However, the spectral indicator provides a better correlation with the speed, showing a clearer trend. Moreover, there is an evident influence of the lubricant, resulting in differences among the band slopes.

6.2. Temperature effects and AE

6.2.1. Test 2a: Standard-range die temperature influence

Test 2a consists in a cut-off of the refrigerant flow during wire drawing at stationary speed. The cut-off is performed after a line warm-up to avoid other perturbations. This procedure generates an increase in the die temperature until a warning temperature is reached, considering that the test is developed in a standard-range below critical operation. After this temperature is reached, the refrigeration is opened again to finalize the test.

The die temperature increment, as a result of the cooling flow cut-off, provokes a reduction of AE amplitude as its shown in Fig. 13. This graph displays the AE signals RMS with the die box temperature and the drawing speed.

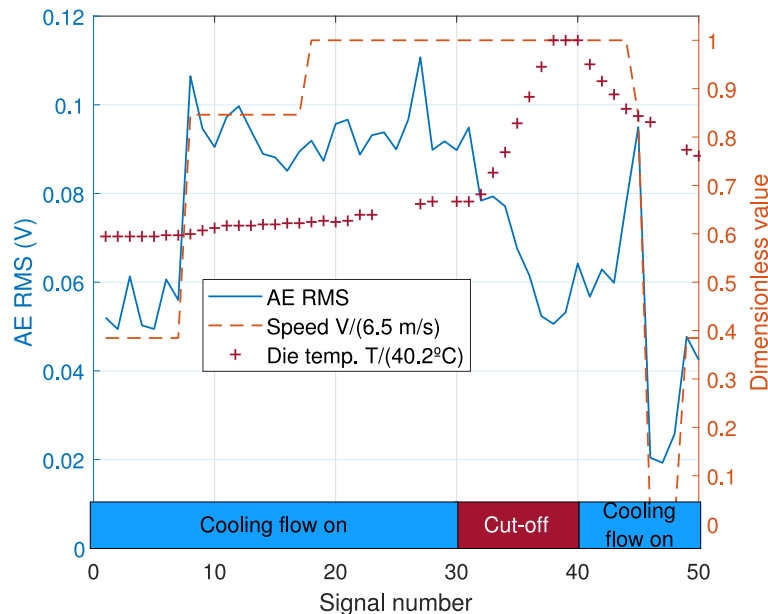


Fig. 13. AE RMS level during the cooling flow cut-off and dimensionless operational parameters of die box temperature and drawing speed (Test 2a).

In the next acquired signal after the cut-off (after two minutes), the AE RMS suffers a 14% reduction. Furthermore, die box temperature presents a slight increment of 8% from 26.8 °C to 29.2 °C, both temperatures far below critical values, compatible with normal refrigerated operation. In the last acquisition before restarting the cooling flow, when the die box reaches 40 °C, the AE RMS decreased 45%. In addition to the AE sensitivity to cooling conditions, it responds faster than the temperature measured in the die box surface, reducing its level drastically and with a quicker response.

Fig. 14 shows the corresponding spectral evolution during same cooling cut-off test. The AE amplitude reduction is meaningful in a mid-low frequency band corresponding to 25–125 kHz. As heating progresses, the spectral decrease is observed for all spectrum, also reducing the sensor resonant frequency peak amplitude.

On the other hand, Fig. 15 represents the evolution of the AE spectral indicator for the three selected bands of low, medium and high frequency. This indicator allows to represent with a significant data reduction what is observed in the evolution of the spectrum (Fig. 14) adding information to what is observed only with the RMS (Fig. 15). The 55–150 kHz band has a more pronounced relative reduction, and the reduction is also observed for 150–300 kHz band. The low frequency band, 25–55 kHz, is reduced, although due to its lower value, this behaviour is less noticeable.

The origin of the increase in temperature is caused, in the first instance, by reducing the heat exchange out of the system rather than by increasing friction or plastic deformation, aspects that may be subsequent consequences. Therefore, this short-time experiment, below a critical die box temperature (warning alarm set at 40 °C), can be considered as good drawing conditions without negative effect in the wire. The resulting wire quality is considered adequate owing to the observed wire surface characteristics and the wire temperature, measured after the cross-section reduction, that maintain similar values independently the overheating in the die.

The AE amplitude reduction is not evidenced in other scenarios than reducing the drawing speed, when all other parameters remaining unchanged. Consequently, the AE amplitude reduction is result of the overheating mainly due to aspects related with

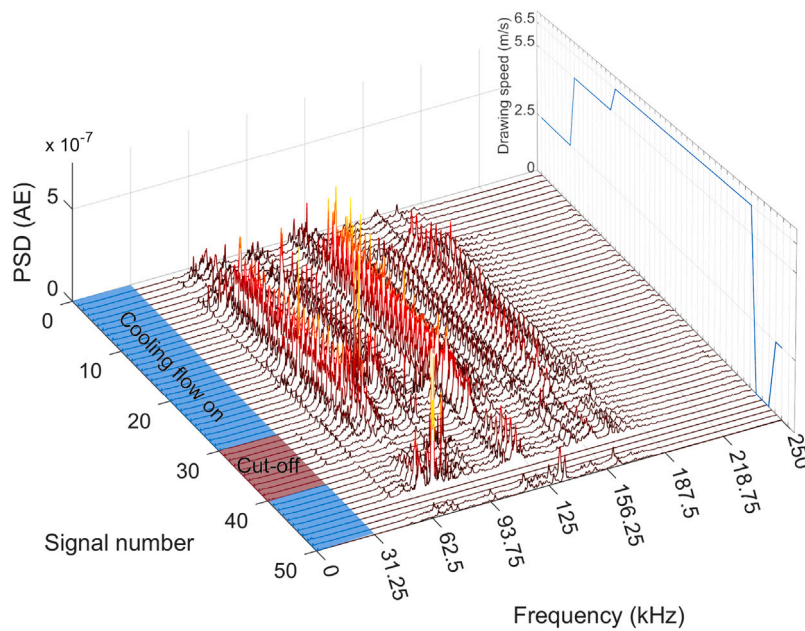


Fig. 14. AE spectral evolution during the cooling flow cut-off (same signals than Fig. 13, Test 2a).

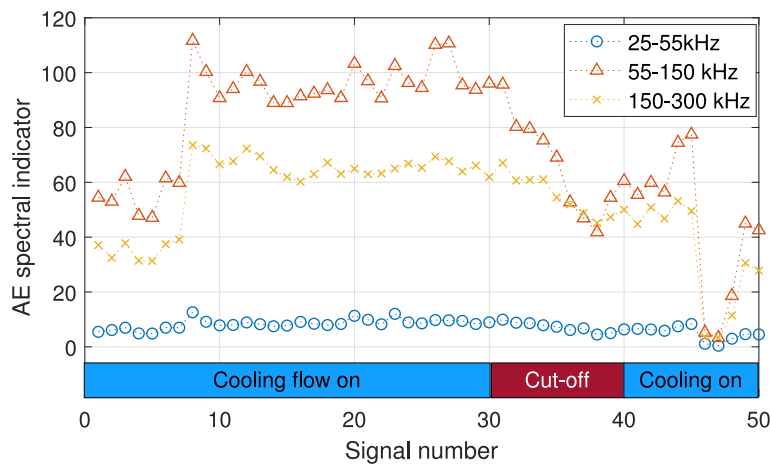


Fig. 15. AE spectral indicator during the cooling flow cut-off (Test 2a).

the lubricant working point modification. This modification affects varying the reactivity and the properties of the resulting lubricant-coat reacted compound.

As a result of this experiment, it has been suggested the employment of AE signals to optimize the working temperature by controlling the heat exchange. Current procedure consists of cooling as much as the water temperature is able, without a fixed working point, which, in turn, can be modified by variations in the environmental conditions. Nevertheless, an excessive temperature leads to reduce wire quality and to other malfunctions, hence a diminution of AE amplitude cannot always be related with better drawing conditions.

6.2.2. Test 2b: Out-of-range die temperature influence

Test 2b consists in a cut-off of the refrigerant flow, but exceeding the warning die box temperature, providing additional results to the previous test.

Fig. 16 displays the AE RMS and the die box temperature, for reels drawn at its nominal stationary speed of 5.5 m/s (reel 1, point A to B) and the second at 6.5 m/s (reel 2, point B to D). First reel is drawn before the cut-off, as reference of stationary operation conditions with a similar wire product. The second reel is completely drawn without refrigeration in the last stage die

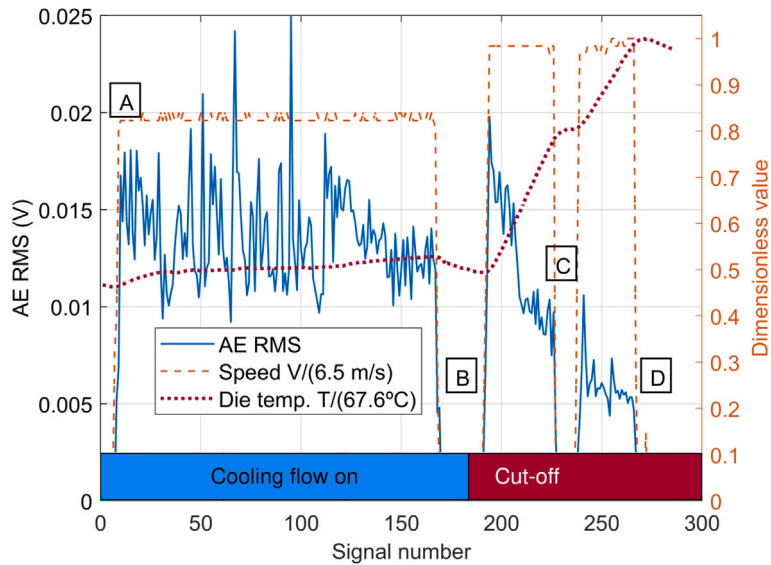


Fig. 16. AE RMS level and die box temperature during the second cooling flow cut-off test, cut-off starting in point B (Test 2b).

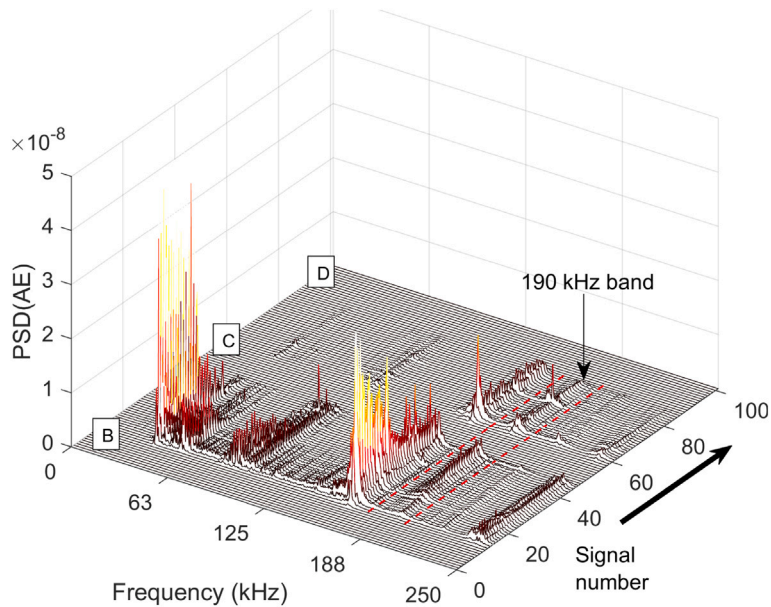


Fig. 17. AE spectral evolution during the second cooling cut-off test (signals corresponding to points B-D in Fig. 16, Test 2b).

box. Therefore, AE RMS related to cooling cut-off is represented between points B and D. The zero level in AE RMS at point C represents a line stoppage to deactivate the automating warning system that stops the line.

The spectrum evolution during the cooling flow cut-off is shown in Fig. 17 (corresponding B-D points in Fig. 16). Globally, the spectra display a progressive decrease as the temperature increases. Ending test signals apparently disappear in reference with the starting levels, only the content at the sensor resonant frequency (150 kHz) remains observable at that scale due to the higher sensitivity.

The effect of the extreme temperature seems to be evidenced by the opposite trend in the 190 kHz band. This peak around 190 kHz, with lower magnitude in the spectrum, but significant AE content (due the lower sensor response at this frequency), is observed with a slight increasing progression in the first half of the test that remains visible in the second half. The initial observation of this peak coincides with a drastic reduction of the global RMS level, mainly in the low frequency, observed in the RMS step down between B-C points in Fig. 16 and disappearance of the frequency peak at 30 kHz in Fig. 17.

The spectral indicator is displayed in Fig. 18 shows similar information than the spectrum (shown in Fig. 17) with less output data. After point B, when the cooling flow cut-off is performed, both low and mid frequency bands exhibit a descending trend with the temperature increment, as observed with RMS (Fig. 16). The mid frequency band contains part of the sensor resonant zone, hence the lower reduction for 55–150 kHz in the indicator with respect to the previous reel drawing (between points A-B). On the other hand, the 150–300 kHz band drastically increases, overpassing the 55–150 kHz band after the point C. Therefore, the high frequency increment, mainly in the 190 kHz band, is registered through the spectral indicator.

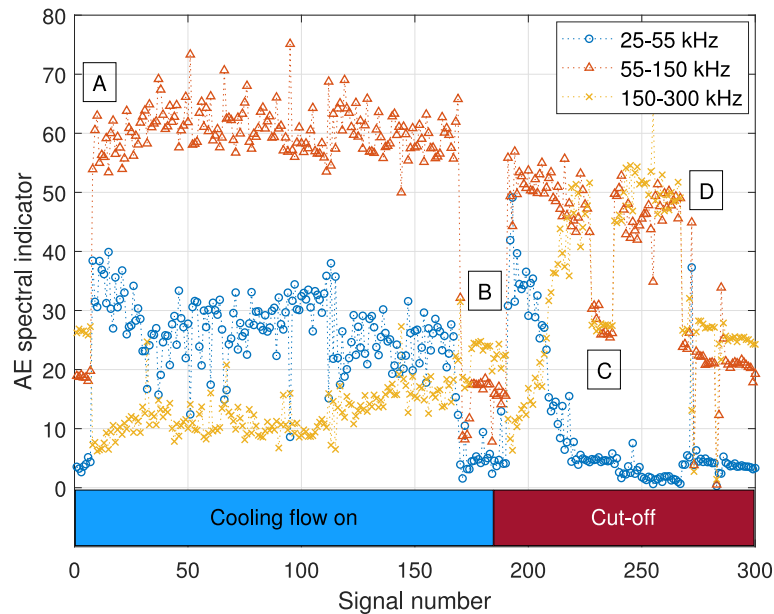


Fig. 18. AE spectral indicator during Test 2b (same signals than Fig. 16).

In contrast to Test 2a, the extreme temperature has provoked a reaction of the phosphate coating that results in wire delamination, visible in the debris presence in Fig. 19. Hence, this reel was considered as a damaged product.



Fig. 19. Carbonized debris disperse around the die box bench form the delaminated phosphate layer waste due to the die overheating (Test 2b).

The AE amplitude continues with a global decreasing in spite of that problem. However, the slight increasing progression in the 190 kHz peak, opposite to the overall behaviour, could be related with that phenomenon, as it is the only deviation observed in the spectrum tendency with respect to refrigerated conditions. By pushing the temperature conditions to the limit, its relation with AE amplitude, observed in standard-range (Test 2a) is confirmed. The coating delamination adds indications of the AE dependence on lubrication conditions and lubricant reactivity, as the spectral analysis reveals.

6.3. Drawing die degradation and AE

6.3.1. Test 3a: Influence of the reel

It has been mentioned that different wire material supposes different conditions due to the different contact behaviour related with the wire characteristics. Test 3a corresponds to the monitoring of consecutive reels drawn at a same cross-section reduction ($S_i/S_f = 2.30$) and same nominal drawing speed (5.5 m/s), during approximately 20 h of standard operation. Fig. 20 shows the spectral evolution of AE signals acquired periodically during this drawing activity of same wire product.

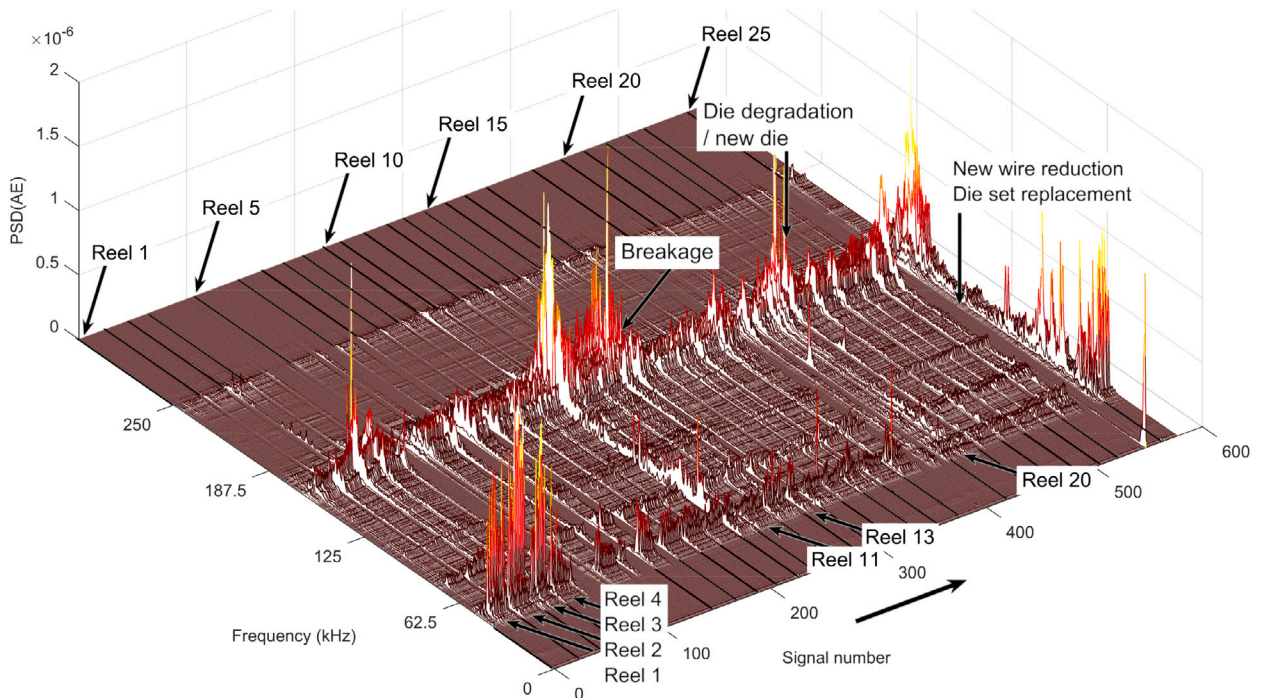


Fig. 20. AE spectral evolution during the drawing of successive reels of same wire product, or same reduction and inlet wire material (Test 3a).

First four reels (Reel 1–4 in Fig. 20) are characterized by high amplitude peak in the low frequency band, around 50 kHz. The lower sensor sensitivity in that frequencies implies the higher AE waves intensity exciting this band, whose spectral peak exceeds the amplitude corresponding to the peak at the sensor resonant frequency. The 50-kHz-band decays in amplitude progressively along the drawing time. On the other hand, higher frequency excitations, represented by the 150 kHz band, increase their peak amplitude during the initial four reels.

These modifications in the spectra are related with the initial wear of the set of new dies, installed with the respective geometry for the necessary reduction in every stage of the drawing line. Initial behaviour after a new drawing line set-up starts at lower temperatures, as usually happens due to longer stoppage time for proper installation. Low temperatures in the wire-die interface affects the lubricant response, modifying the surface contact with respect to those in warm-up operation. Initial wear and warm up are present at new wire products, however, that behaviour does not imply damage or an incidence beginning. Generally, the starting drawing speed is incremented gradually to the nominal to avoid problems in that scenario.

The progression of the wire drawing continues with stable values in the following reels until signals 225–300 in Fig. 20, corresponding to reels 11–13. After this point, the resonant frequency peak increments its amplitude. This ends in a wire breakage which terminates the production of the reel number 13. Wire breakage occurs apparently in a random way and the wire is threaded again to continue the manufacturing. Nevertheless, the increased peak amplitude in the AE could be pointing negative contact that leads to this breakage.

After this incident, the drawing continues until a noticeable degradation of the die is registered during standard inspection. The wear suffered by the die is observed through wire diameter measurements slightly out of tolerance. This measurement is registered

after reel 20, corresponding with signal number 450 in Fig. 20. The spectra preceding the critical wear in the die are characterized by an increasing amplitude of the resonant frequency peak that reach a maximum at the end. This particular case corroborates similar increments of spectrum peak amplitude observed in other periods under die wear. In this case, no significant content is observed in the low frequency bands.

After this incidence, drawing restart with a new die of same reduction, manufacturing five more reels until the desired wire length is completed and the drawing line is modified for a different wire section. Initial wear does not show a significant progressive increment in the spectra due to the starting higher temperatures for the replaced die. The spectral pattern of these reels is similar to the obtained with the previous die, with some differences in the excited peaks between 50–150 kHz.

The last spectra showed in this figure (Fig. 20) corresponds to a new wire production of different cross-section. It is represented here as a demonstration of the change in the spectral pattern. The amplitude and the spectral distribution is clearly different, displaying the identification of a reel at different reduction which is detailed in the next test (Test 3b).

Fig. 21 presents the spectral indicator corresponding to Test 3a.

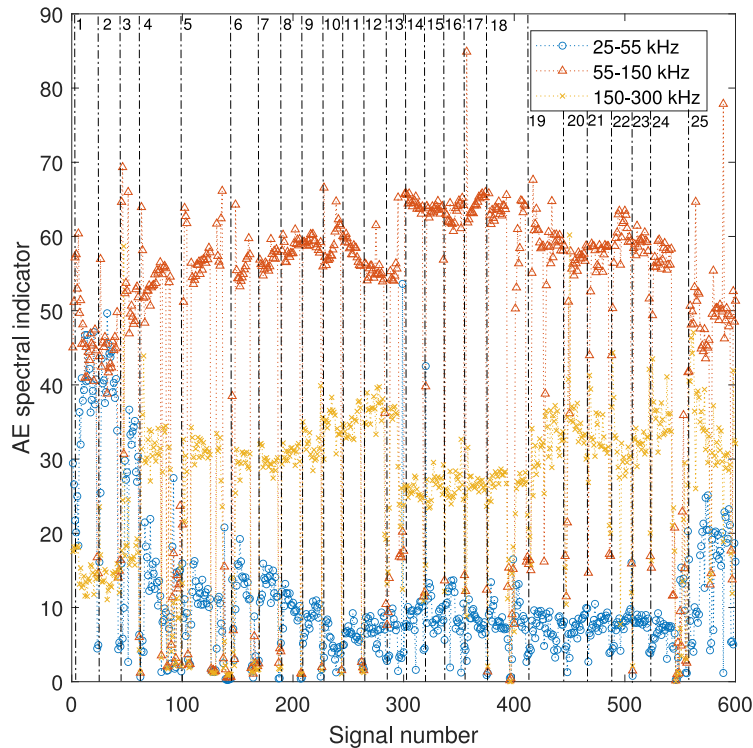


Fig. 21. The AE spectral indicator evolution during the drawing of successive reels of same wire product, showing the start point and corresponding reel number in this sequence (Test 3a).

The initial higher level in the 50 kHz peak of the spectrum and its progressive reduction during the four first reels is shown by the higher value in the 25–55 kHz spectral indicator (signals 0–100). Moreover, the breakage appears as a progressive increase of 150–300 kHz band until signal 300, obtaining distinguishable indicator values after this incidence. Also the die degradation is observed as an increment of the 150–300 kHz band prior to the signal 450, when the degradation is noticed.

6.3.2. Test 3b: Influence of cross-section reduction

Test 3b evaluates through monitoring data the cross-section reduction (CSR) influence in the AE signals. Starting a new wire product, with different CSR, obliges to modify the dies in the multiple stages composing the drawing line. Fig. 22 displays the spectral content distribution with a colourmap-type graph of successive reels drawn at different CSR. Each signal spectrum is normalized dividing by its spectrum mean value to obtain same amplitude range, therefore, the frequency distribution of the peaks can be easily comparable for different amplitude signals.

Amplitude variation is related with the variation of the parameters defining the production. The different CRS, wire material and set of dies modifies its value, obtaining various amplitude ranges in the AE signals. No evident relation is observed, focusing the analysis in the peak amplitude distribution along the frequency spectrum. Because of this, signal spectrum normalization is performed. According to what was observed in the previous study within one reel, modifications in the speed affect globally the spectrum rather than increase or decrease specific frequencies. In this test, drawing speed is stationary and approximately maintained at 5.5 m/s for all the reels, hence no significant effect of this parameter in the amplitude.

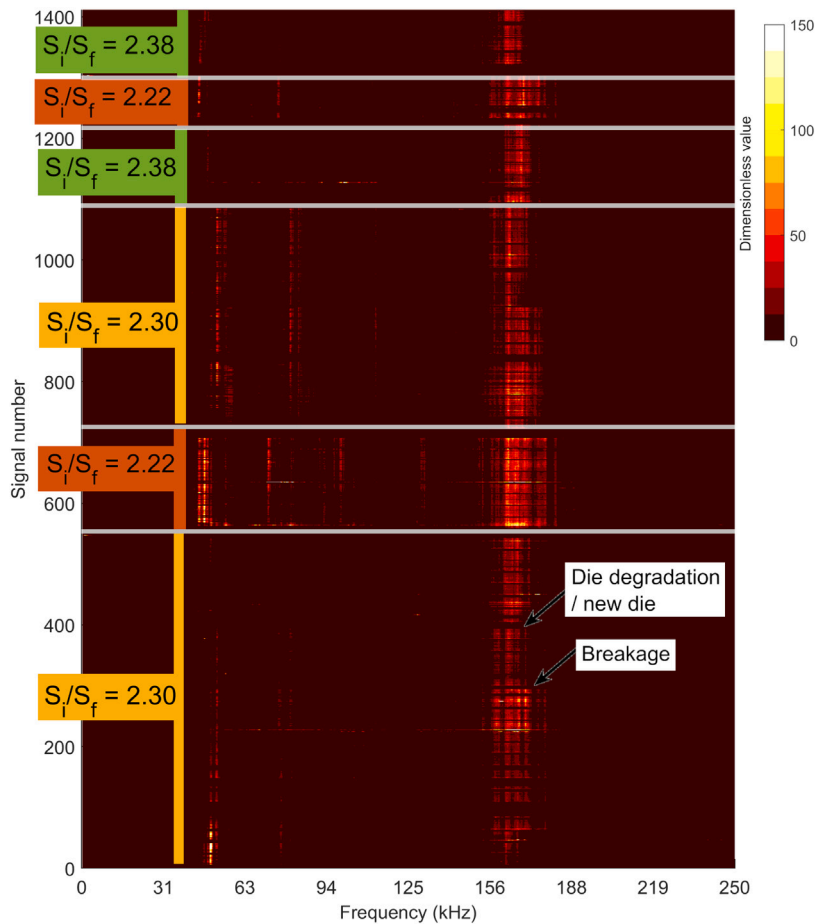


Fig. 22. AE spectral evolution for long term production (Test 3b) showing spectral patterns for different cross-section reduction (S_i/S_f initial/final section), starting by the signals in Fig. 20.

The signals spectra in the colourmap graph (Fig. 22) involve six successive sequences of reels drawn at CSR: 2.3 (corresponding with same reels than Fig. 20), 2.22, 2.30, 2.38, 2.22 and 2.38 respectively. For these results, the AE main excited frequency bands depend on the die and, therefore, in the global wire reduction, obtaining a different pattern in the spectral amplitude distribution.

After the first wire product at 2.30, a new wire is drawn at a total CRS of 2.22. Initial wire cross-section is the same than previous, hence less reduction is applied. As a result of changed wire material, operating conditions and dies different geometry, a higher global amplitude for the AE spectrum is obtained. In addition, a new distribution in the frequency bands is observed.

The next cross-section reduction in the reel sequence (Fig. 22) is the initial one ($S_i/S_f = 2.30$). As a result, the spectral pattern returns to a similar distribution than the observed during the previous operation (same speed of 5.5 m/s). After that, two more reduction changes are registered, varying to 2.38, 2.22 and 2.38 again. Once again, the distribution of the peaks in the spectrum correlates with the CSR imposed on the wire, with similar patterns being observed for the same reduction. Additionally, it can be observed that the higher the reduction ratio, the narrower the frequency band affected around 150 kHz is.

6.3.3. Test 3c: Influence of reel with different drawing speed

The effect of drawing speed is incorporated into the AE analysis in conjunction with wire material and cross-section reduction variations in Test 3c. Fig. 23 shows the AE RMS for four different reels with diverse characteristics (non-controlled in the monitored process). Two reels (1 A & 2 A) are presented for same CRS A ($S_i/S_f = 2.22$) and another two (1B & 2B) for the CRS B ($S_i/S_f = 2.30$), all of them manufactured from different wire material. The signals were obtained at three stationary speeds of 2.5, 5.5 and 6.5 m/s.

The AE RMS results higher for 5.5 m/s than the corresponding to 2.5 m/s for all reels, increasing its value with the speed. However, when the speed is increased to 6.5 m/s, different behaviour is observed: for Reel 1 A, the highest RMS is obtained at 6.5 m/s meanwhile in Reel 2 A the maximum is exhibited at 5.5 m/s. Analogous divergent behaviour is displayed for reels 1B & 2B, drawn at same CRS, but also different RMS tendency at high drawing speed. It is evidenced that a limit in the relationship between AE amplitude and drawing speed exists depending in the wire material.

This limit depends of wire characteristics that are not considered in this research, nevertheless, industry operators establish nominal working speed under that limit for different metal castings and wire characteristics, knowledge obtained through trial and error. In this regard, AE signals could provide a reference level to optimize the speed, establishing the adequate speed in terms of the RMS.

During standard factory production different reels, sections and speeds are combined, as a result of an *a priori* selection of the parameters that are considered most appropriate. Nonetheless, excessive drawing speed for a reel could lead in a rough operation and the occurrence of incidents.

Fig. 24(a) displays the “reel averaged RMS” values for the reels produced consecutively (a total of 266 reels at 4 different CSR of 2.22, 2.29, 2.30 and 2.38). This indicator is calculated as the average of the RMS value of all records acquired during the interval during a reel is produced. Since the AE signals, in the time and spectral domain, do not present mayor dispersion within a single reel, indicators averaged over its production can be representative for an overall description of the reel and incident identification. Therefore, an averaged indicator can be calculated grouping the signals acquired during the reel manufacturing.

The RMS is represented versus the mean drawing speed (in this case a range from 4.3 till 6.09 m/s) and the corresponding applied cross-section reduction is shown in the legend (Fig. 24(a)). For the AE RMS, the values fluctuate between 0.25 and 1.25 V, but for the CSR $S_i/S_f = 2.30$ several reels exhibit higher amplitude for 5.5 m/s speed.

Apparently, no tendencies are observed in this scattered data set. To analyse a possible relation between AE RMS and the drawing speed of the reels, mean value and standard deviation are shown in Fig. 24(b). The values are grouped in speed bands of 0.25 m/s and separated by the corresponding cross-section reduction. As a result, same conclusion is reached, no tendency among AE amplitude, speed and reduction can be established.

In summary, spectral content in the signals and its evolution (as presented in Figs. 20 and 22) reveals an accurate response when die geometry (or CSR) is modified. However, averaged values in the time domain signals, as RMS (Fig. 24(a)), fluctuate, not

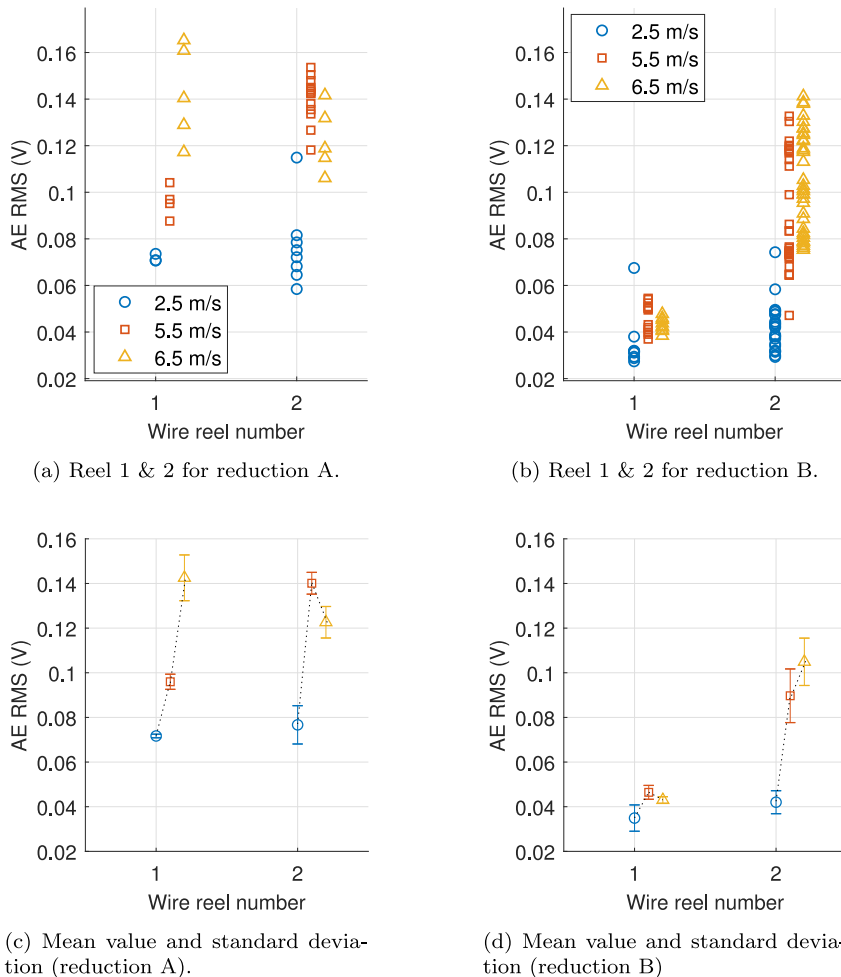
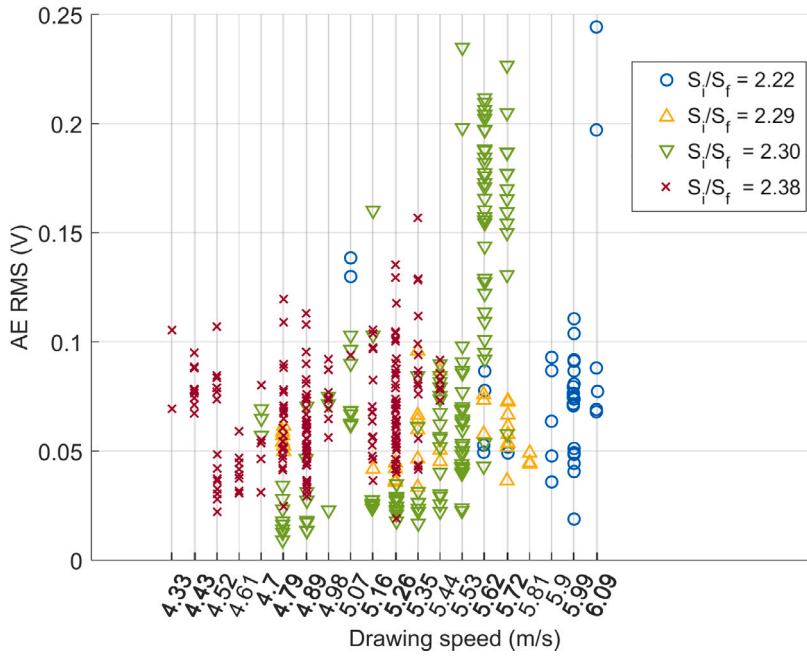
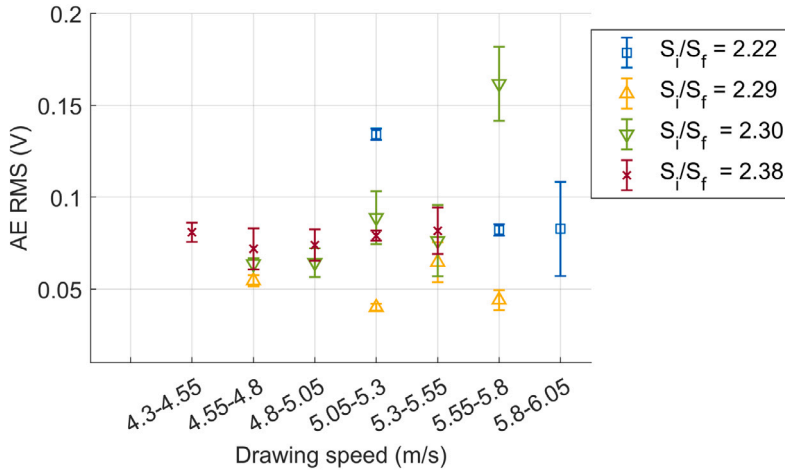


Fig. 23. AE RMS from four reels of different characteristics at same three stationary drawing speeds for two different cross-section reduction (Test 3c).



(a) Reel-averaged AE RMS.



(b) Mean value and standard deviation by speed band of reel-averaged AE RMS.

Fig. 24. Reel averaged AE RMS represented versus drawing speed and cross-section reduction for the reels produced during one month (Test 3c).

providing a clear trend in respect to the applied section reduction or the drawing speed. This averaged approach may be useful for long-term characterization of the operation but it is not conclusive in interpreting the short-term status, losing valuable information in the slight variations between signals. The setting of the drawing speed based on the experience accumulated by the industry, selected according to the characteristics of the wire being produced, would be behind this apparent lack of correlation between AE signal level and section reduction.

6.3.4. Monitoring of standard production

The previous analysis displays the effect of the parameters variation, keeping the rest unchanged, in the AE signals. As one reel, or consecutive same wire product reels, are drawn with the same die set, deviation from the spectral signature is unexpected unless the drawing die varies its properties, for example, due to wear, reporting an incident.

As an example of the drawing monitoring, Fig. 25 shows the spectral evolution of ten consecutive reels where an incidence was detected. The analysis of the spectrum variation allows to interpret what is happening on the line and the interaction between wire and die.

The spectra of first four reels (Fig. 25) display a stable signal response without significant variations, either in excited frequency bands or their amplitude, until the dies and the inlet wire material are replaced. The drawing dies replacement was pre-set with no wear detected at that time, considering in this case the replaced components in good conditions.

After the new die is changed, two reels are drawn consecutively (Reels 5 and 6) until a stoppage is produced (Fig. 25). The spectral pattern differs due to the dies geometry and the different wire metal casting. Those reels spectra present a decreasing trend in the peak amplitude, mainly evidenced around 150 kHz band. This response is linked with new die operation when the line is already warmed-up and die temperature increases (similar response than Test 2a), observed in analogous periods non related with incidences. After this, a longer than usual line stoppage occurs, not associated with a problem in the wire drawing, but related to the origin of the incident subsequently detected. The analysis of the occurrence, carried out *a posteriori* in the current study, would reveal in real-time the beginning of the incident as is detailed next.

Subsequent post-stoppage operation leads to wire damage progression as an increasing peak amplitude in the last four reels (Fig. 25). Frequency bands of 50–100 kHz and 150 kHz (AE sensor resonant frequency) are greatly affected. Four complete reels are manufactured with this observed trend until an operator detected the damaged surface, almost out-of-tolerance, of the last reel presented in this sequence. This wire damage was eventually attributed to the die wear after the post-incident inspection, seeded due to poor lubricant impregnation during the prolonged stoppage. At this stoppage, the lubricant was exposed to high humidity, which prevented the wire from being properly impregnated, obtaining a close-to-unlubricated conditions. AE signal variations are attributed to the worsening of contact conditions.

Fig. 26 presents the AE spectral indicator for this test. The reels after the new die, installed between Reels 4 and 5, display a different frequency distribution denoted as a higher level of the indicator for the 150–300 kHz band. Nevertheless, the global increment in the peak amplitude maintains the indicator values. Only during the last reel a different tendency is observed, showing a decrease of the 55–150 kHz band in parallel to an increment in 150 kHz.

In this case, the AE spectral indicator, useful in several operating conditions, reveals an overall description of manufacturing behaviour, but less accurate than spectrum. That limitation regarding the spectral could be solved by the indicator reformulation in further research. However, it is observed in this test that when there is decrease of the indicator in the medium frequency band and simultaneously an increment of the high band values, an incidence occurred. This trend was observed also in Test 2b and 3a (Figs. 18 and 21).

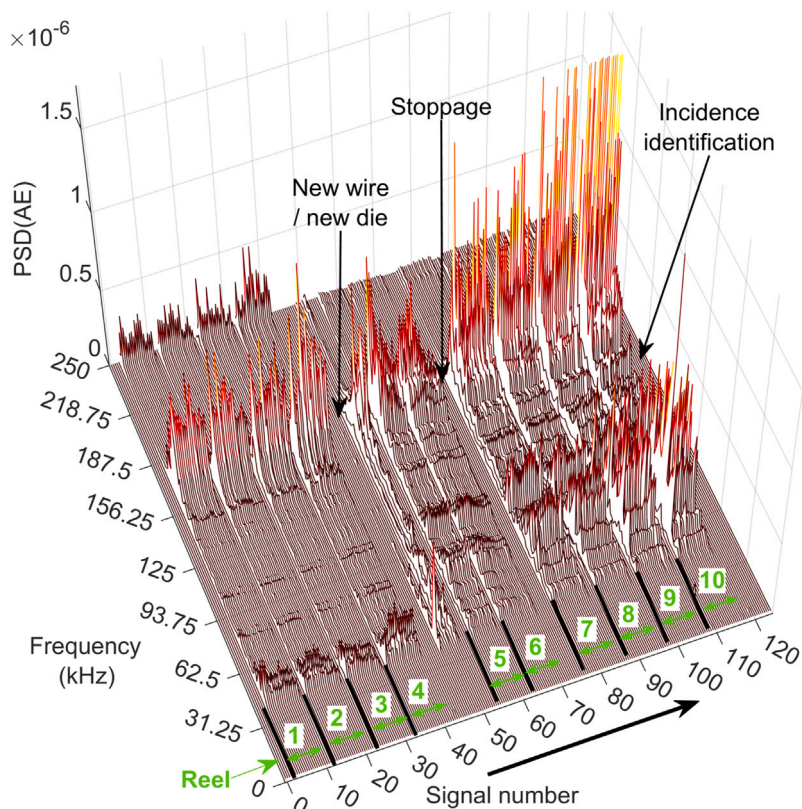


Fig. 25. AE spectral evolution during production incidence consisting on die wear progression and subsequent wire damage.

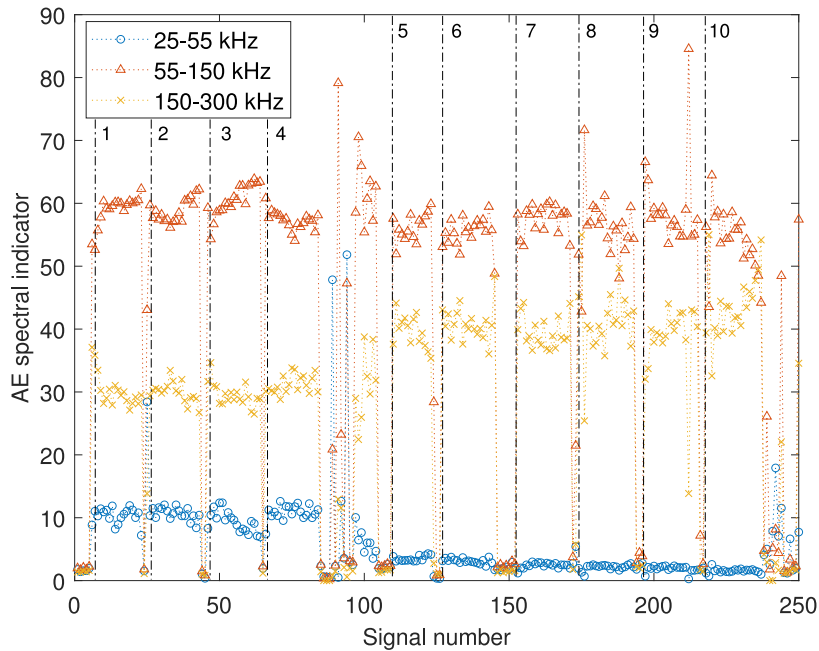


Fig. 26. AE spectral indicator during the test in real conditions (same signals than Fig. 25).

7. Conclusions

AE signals have revealed a high sensitivity to the variation of analysed wire drawing operational parameters. Several aspects have been evaluated in the experimental study, obtaining information about the process by means of the AE signals: AE signal has been studied in time and frequency domain, including the use of indicators in both domains to interpret the signals with a significant reduction of output data.

Although there is an interdependence between the factors describing wire drawing, some conclusions and trends in their variation have been identified. For instance, a modification in wire drawing speed has an effect on the AE. In general, faster drawing of same wire provides higher AE amplitude. Nevertheless, the response and the limits for a valid relationship between them depends on more factors than the considered. This is the case for the utilization of different lubricants, that modifies the AE signal amplitude and the tendency between AE and speed, when same wire (same material characteristics and contact behaviour) is considered. The results were obtained with two different lubricant types, based on calcium and sodium soap. However, the response depends on more factors, as has been shown by the repetition of the test with another reel, obtaining an inverse amplitude response. That reveals the high AE sensitivity to the process, allowing to differentiate the operation with both lubricants.

On the other hand, a die temperature increase corresponds to a decrease in AE amplitude. These results have been verified by repeating the tests with different wires. The temperature in the die is not a control parameter of the process but its relevance should be considered. According to the observations, the AE could serve as an indicator to set the optimum temperature for lubricant, wire and die, controlling the cooling flow.

The AE originating from the wire-die interaction shows a high frequency spectrum pattern related with the physical mechanisms taking place in the contact area and the wire material. The microscopic scale phenomena release AE energy at different wideband frequencies. Assuming the invariance of working conditions, modifications in the AE can be related with changes in the drawing interaction, mainly affected by transitory lubrication regime and wear progression. In turn, if that modifications excite different frequency bands, their effect could be appreciated separately in the spectra.

Another important aspect comes from the evolution of the die, an element liable to wear and tear, which is changed in order to use the appropriate geometry for a specific reduction in section is desired. AE signals, in particular by means of their frequency spectrum, show patterns that remain unchanged as long as there are no changes in the process. The exchange of the die modifies the spectral pattern and damage in its active surfaces can be observed as trends in the spectral amplitude in certain frequency bands of the spectrum.

In terms of wire drawing monitoring, the frequency analysis is observed as a more advantageous tool than the study of the time domain signals. The computational cost and the need of an experienced supervisor to examine the spectrum can be overcome, as proposed in an preliminary approach in this work, through a condition indicator. In this regard, the AE spectral indicator revealed a refined representation of the operational behaviour than the RMS with equivalent memory data storage. An interesting example is the observed simultaneous, but opposite, tendency preceding certain incidents, the decrease of the medium and increment of the high frequency bands. The variations in the low, mid and high frequency bands respond quite well to the modifications in the

process behaviour that could be related with contact and wear phenomena, that should be studied in controlled tests. Although, a further research on the contributions in the spectrum frequency bands is proposed as the next step in this line of research to refine the indicator.

In conclusion, it is necessary to isolate variables involved in the lubricated contact of asperities, including plastic deformation and the synergy between wire coating and lubricant, in order to propose a model. Due to the complexity of the process, it is proposed further experiments in simplified wire drawing facilities for the better comprehension. Nevertheless, the assessed evaluation for the application of AE monitoring for wire drawing process reveals its promising usefulness.

Declaration of competing interest

The authors declare that they have no known competing financial interests or personal relationships that could have appeared to influence the work reported in this paper.

Data availability

The data that has been used is confidential.

Acknowledgements

This work was financially supported by the Spanish Ministry of Science and Innovation (MICINN) [grant numbers PID2020-116213RB-I00, PRE2018-083538, DPI2017-85390-P]. The authors would like to shown their gratitude to the wire manufacturer “TYCSA-PSC” (GLOBAL SPECIAL STEEL PRODUCTS, S.A.U.) for providing the facilities employed for the experimental tests under the project “*Mejora del proceso de trefilado mediante el monitorizado de señales dinámicas (METRE)*”.

References

- [1] J. García-Martín, J. Gomez-Gil, E. Vázquez-Sánchez, Non-destructive techniques based on eddy current testing, *Sensors (Basel Switzerland)* 11 (2011) 2525–2565.
- [2] Foerster Institut, Deutschland | Institut Dr. Foerster GmbH und Co. KG, 2022, Accessed: 2022-10-17.
- [3] ISEND, WIRE - ISEND nondestructive testing solutions for wire, 2022, Accessed: 2022-10-17.
- [4] B. Nilsson, B. Stenlund, Detection of lubrication failures in wire drawing, *Wire Ind.* 51 (611) (1984) 855–858.
- [5] T. Holm, K.E. Karlstrom, A. Philipson, B. Nilsson, Lubrication failures in wire drawing, *Wire Ind.* 611 (51) (1985) 242–245.
- [6] M.M. Stopa, B.J. Cardoso-Filho, Online torque and drawing force estimation in wire drawing process from electric motor variables, *IEEE Trans. Ind. Appl.* 44 (3) (2008) 915–922.
- [7] L. Pejryd, J. Larsson, M. Olsson, Process monitoring of wire drawing using vibration sensing, *CIRP J. Manuf. Sci. Technol.* (2017).
- [8] J. Larsson, A. Larsson, L. Pejryd, *Wire 4.0.pdf*, *Wire J. Int.* (2020) 58–63.
- [9] J. Larsson, A. Jansson, L. Pejryd, Process monitoring of the wire drawing process using a web camera based vision system, *J. Mater. Process. Technol.* (2017).
- [10] J. Larsson, A. Jansson, P. Karlsson, Monitoring and evaluation of the wire drawing process using thermal imaging, *Int. J. Adv. Manuf. Technol.* 101 (5–8) (2019) 2121–2134.
- [11] N.C. Pease, Flaw detection in wire drawing, 1983, Patent GB2137344A.
- [12] S. Ramalingam, D.A. Frohrib, Integral acoustic emission sensor for manufacturing processes and mechanical components, 1989, University of Minnesota, Patent US4927299A.
- [13] QASS, Wire drawing - condition monitoring for your process, 2022, Accessed: 2022-10-17.
- [14] S. Masaki, T. Tabata, K. Konishi, Evaluation of lubrication in wire drawing using acoustic emission method, *J. Jpn. Soc. Technol. Plast.* 295 (25) (1985) 835–841.
- [15] M.Y. Choi, W.G. Lee, J.D. Park, Acoustic emission monitoring fine wire drawing process, *J. Korean Soc. Mach. Tool Eng.* 3 (1996) 43–50.
- [16] E. Kannatey-Asibu, E. Emel, Linear discriminant function analysis of acoustic emission signals for cutting tool monitoring, *Mech. Syst. Signal Process.* 1 (4) (1987) 333–347.
- [17] A.A. Houshmand, E. Kannatey-Asibu, Statistical process control of acoustic emission for cutting tool monitoring, *Mech. Syst. Signal Process.* 3 (4) (1989) 405–424.
- [18] I. Buj-Corral, J. Álvarez-Flórez, A. Domínguez-Fernández, Acoustic emission analysis for the detection of appropriate cutting operations in honing processes, *Mech. Syst. Signal Process.* 99 (2018) 873–885.
- [19] W. König, K. Kutzner, U. Schehl, Tool monitoring of small drills with acoustic emission, *Int. J. Mach. Tools Manuf.* 32 (4) (1992) 487–493.
- [20] C.E. Everson, S.H. Cheraghi, The application of acoustic emission for precision drilling process monitoring, *Int. J. Mach. Tools Manuf.* 39 (3) (1999) 371–387.
- [21] W. König, Y. Altintas, F. Memis, Direct adaptive control of plunge grinding process using acoustic emission (AE) sensor, *Int. J. Mach. Tools Manuf.* 35 (10) (1995) 1445–1457.
- [22] J.S. Kwak, J.B. Song, Trouble diagnosis of the grinding process by using acoustic emission signals, *Int. J. Mach. Tools Manuf.* 41 (6) (2001) 899–913.
- [23] E. Susič, I. Grabec, Characterization of the grinding process by acoustic emission, *Int. J. Mach. Tools Manuf.* 40 (2) (2000) 225–238.
- [24] V. Pandiyan, W. Caesarendra, T. Tjahjowidodo, H.H. Tan, In-process tool condition monitoring in compliant abrasive belt grinding process using support vector machine and genetic algorithm, *J. Manuf. Process.* 31 (2018) 199–213.
- [25] I. Marinescu, D.A. Axinte, A critical analysis of effectiveness of acoustic emission signals to detect tool and workpiece malfunctions in milling operations, *Int. J. Mach. Tools Manuf.* 48 (10) (2008) 1148–1160.
- [26] J.A. Duro, J.A. Padget, C.R. Bowen, H.A. Kim, A. Nassehi, Multi-sensor data fusion framework for CNC machining monitoring, *Mech. Syst. Signal Process.* 66–67 (2016) 505–520.
- [27] X. Li, A brief review: acoustic emission method for tool wear monitoring during turning, *Int. J. Mach. Tools Manuf.* 42 (2) (2002) 157–165.
- [28] A. Iturrospe, D. Dornfeld, V. Atxa, J.M. Abete, Bicepstrum based blind identification of the acoustic emission (AE) signal in precision turning, *Mech. Syst. Signal Process.* 19 (3) (2005) 447–466.

- [29] M.S.H. Bhuiyan, I.A. Choudhury, M. Dahari, Monitoring the tool wear, surface roughness and chip formation occurrences using multiple sensors in turning, *J. Manuf. Syst.* 33 (4) (2014) 476–487.
- [30] S. Rangwala, S. Liang, D. Dornfeld, Pattern recognition of acoustic emission signals during punch stretching, *Mech. Syst. Signal Process.* 1 (4) (1987) 321–332.
- [31] S. Hao, S. Ramalingam, B.E. Klamecki, Acoustic emission monitoring of sheet metal forming: characterization of the transducer, the work material and the process, *J. Mater. Process. Technol.* 101 (1) (2000) 124–136.
- [32] T. Skåre, F. Krantz, Wear and frictional behaviour of high strength steel in stamping monitored by acoustic emission technique, *Wear* 255 (7) (2003) 1471–1479, 14th International Conference on Wear of Materials.
- [33] B.A. Behrens, S. Hübner, K. Wölki, Acoustic emission—A promising and challenging technique for process monitoring in sheet metal forming, *J. Manuf. Process.* 29 (2017) 281–288.
- [34] E. Susič, I. Grabec, Application of a neural network to the estimation of surface roughness from ae signals generated by friction process, *Int. J. Mach. Tools Manuf.* 35 (8) (1995) 1077–1086.
- [35] E. Dimla, Sensor signals for tool-wear monitoring in metal cutting operations—a review of methods, *Int. J. Mach. Tools Manuf.* 40 (8) (2000) 1073–1098.
- [36] E. Caso, A. Fernandez-del-Rincon, P. Garcia, M. Iglesias, F. Viadero, Monitoring of misalignment in low speed geared shafts with acoustic emission sensors, *Appl. Acoust.* 159 (2020) 1–9.
- [37] E. Caso, A. Fernandez-del-Rincon, P. Garcia, A. Diez-Ibarbia, J. Sanchez-Espiga, An experimental study of acoustic emissions from active surface degradation in planetary gears, *Mech. Syst. Signal Process.* 189 (2023) 1–23.
- [38] A. Hase, H. Mishina, M. Wada, Correlation between features of acoustic emission signals and mechanical wear mechanisms, *Wear* 292–293 (2012) 144–150.
- [39] J.G. Wistreich, The fundamentals of wire drawing, *Metall. Rev.* 3 (1) (1958) 97–142.
- [40] E. Felder, C. Levrau, M. Mantel, N.G. Truong-Dinh, Experimental study of the dry lubrication by soaps in stainless steel wire drawing, in: 4th International Conference on Tribology in Manufacturing Processes, ICTMP, Presses de l'Ecole des Mines de Paris, 2010, pp. 435–444.
- [41] E. Felder, C. Levrau, M. Mantel, N.G. Truong-Dinh, Identification of the work of plastic deformation and the friction shear stress in wire drawing, *Wear* 286–287 (2012) 27–34.
- [42] P. Montmitonnet, M. Brison, F. Delamare, Metallic soap lubrication in wire-drawing: A thermopseudoplastic model, *Wear* 77 (3) (1982) 315–328.
- [43] N. Bay, The state of the art in cold forging lubrication, *J. Mater. Process. Technol.* 46 (1) (1994) 19–40.
- [44] S.M. Byon, S.J. Lee, D.W. Lee, Y.H. Lee, Y. Lee, Effect of coating material and lubricant on forming force and surface defects in wire drawing process, *Trans. Nonferr. Met. Soc. China (Engl. Ed.)* 21 (SUPPL. 1) (2011) s104–s110.
- [45] M. Nilsson, Tribology in Metal Working (Ph.D. thesis), Uppsala University, Department of Engineering Sciences, 2012.
- [46] M.T. Hillery, V.J. McCabe, Wire drawing at elevated temperatures using different die materials and lubricants, *J. Mater. Process. Technol.* 55 (2) (1995) 53–57.
- [47] S. Schnabel, S. Golling, P. Marklund, R. Larsson, The influence of contact time and event frequency on acoustic emission signals, *Proc. Inst. Mech. Eng. J* 231 (10) (2017) 1341–1349.
- [48] M. Akbari, M. Ahmadi, The application of acoustic emission technique to plastic deformation of low carbon steel, *Physics Procedia* 3 (1) (2010) 795–801.
- [49] C. Moon, N. Kim, Analysis of wire-drawing process with friction and thermal conditions obtained by inverse engineering, *J. Mech. Sci. Technol.* 26 (9) (2012) 2903–2911.
- [50] T.H. Kim, B.M. Kim, J.C. Choi, Prediction of die wear in the wire-drawing process, *J. Mater. Process. Technol.* 65 (1–3) (1997) 11–17.
- [51] E.A. Handoyo, A. Hazman, Optimization of wire drawing die's cooling system, *AIP Conf. Proc.* 2001 (1) (2018) 020001.
- [52] K.I. Abe, On the wire drawing lubricant, *Trans. Jpn. Soc. Mech. Eng.* 27 (181) (1961) 1439–1447.
- [53] K.D. Maraité, Ein Beitrag zur Optimierung des halbwarmziehens, stahl und eisen, *Umformtechnische Band* 13 (1988).